# Disordered Euclidean field theory at low-temperature: Two-loop correction in the Distributional Zeta-function approach


Vinicius Lessa da Silva Farinha

**Centro Brasileiro de Pesquisas Físicas**

**Coordenação de Formação Científica**

**Coordenação de Física Teórica**

Rio de Janeiro - RJ


2023

Vinicius Lessa da Silva Farinha

# Disordered Euclidean field theory at low-temperature: Two-loop correction in the Distributional Zeta-function approach

Dissertação apresentada ao curso de Pós-Graduação em Física do Centro Brasileiro de Pesquisas Físicas, como requisito parcial para a obtenção do Título de mestre em Física.

Orientador: Nami Fux Svaiter

Rio de Janeiro - RJ

2023

CBPF
Centro Brasileiro de Pesquisas Físicas
SUBORDINADA AO MCTI

MINISTÉRIO DA CIÊNCIA, TECNOLOGIA E INOVAÇÕES

"DISORDERED EUCLIDEAN FIELD THEORY AT LOW-TEMPERATURE: TWO-LOOP CORRECTION IN THE DISTRIBUTIONAL ZETA-FUNCTION APPROACH"

**VINICIUS LESSA DA SILVA FARINHA**

Dissertação de Mestrado em Física apresentada no Centro Brasileiro de Pesquisas Físicas do Ministério da Ciência Tecnologia e Inovação. Fazendo parte da banca examinadora os seguintes professores:

Nami Fux Svaiter – Orientador/CBPF

Luca Moriconi - UFRJ

Rudnei de Oliveira Ramos – UERJ

Rio de Janeiro, 30 de março de 2023.

# Agradecimentos

Gostaria de iniciar agradecendo ao meu orientador Nami Fux Svaiter. Também quero agradecer ao corpo docente do CBPF, em especial ao Sérgio Duarte, que vem me dando ajudas pontuais desde minha graduação. Agradeço também aos meus colegas e amigos, em especial ao Leonardo Santoro, por me ajudar a manter o foco nos objetivos, e ao Gabriel Bezerra, por ajudar a ler este trabalho, e muitos outros. Quero agradecer aos meus pais, Angerlene e Márcio, e aos meus sogros, Célio e Isabel, pelo suporte. Também ao meu irmão Rodrigo e ao meu primo Saulo, pelos momentos de distração. Quero agradecer especialmente à minha namorada Maria Laura, por continuar sendo meu norte e meu refúgio nos momentos difíceis.

Por último, mas não menos importante, quero agradecer à Coordenação de Aperfeiçoamento de Pessoal de Nível Superior pelo apoio financeiro, pois sem ele, este estudo e muitos outros não seriam possíveis.

# Abstract

We investigate the low-temperature behavior of a system in a spontaneously broken symmetry phase, described by an Euclidean quantum $\phi^4_{d+1}$ model with quenched disorder. We study the effects of the disorder linearly coupled to the scalar field, using a series representation for the moments of the partition function. The result of the one-loop approximation for the Euclidean quantum $\phi^4_{d+1}$ model with quenched disorder, obtained using the distributional zeta-function, was extended to the two-loop approximation.

We begin by discussing some aspects of quantum field theory at finite temperature for a clean system in the spontaneously broken symmetry phase at low temperatures. We also introduce a discussion about disordered systems, random fields and the average over realizations of the disorder for extensive quantities. The distributional zeta-function, an alternative method to the replica trick, is presented to demonstrate the contributions to the renormalized squared mass given by both one-loop and two-loop diagrams in this approach.

***Keywords:*** disorder, quenched, euclidean, fields

# Resumo

Nós investigamos o comportamento em baixas temperaturas de um sistema em uma fase de simetria quebrada espontaneamente, descrito por um modelo quântico euclidiano $\phi^4_{d+1}$ com desordem *quenched*. Estudamos os efeitos da desordem acoplada linearmente ao campo escalar, utilizando uma representação em série para os momentos da função de partição. O resultado da aproximação de um laço para o modelo quântico euclidiano $\phi^4_{d+1}$ com desordem *quenched*, obtido usando a função zeta distribucional, foi estendido para a aproximação de dois laços.

Começamos discutindo alguns aspectos da teoria quântica de campos em temperatura finita para um sistema limpo na fase de quebra espontânea de simetria em baixas temperaturas. Também introduzimos uma discussão sobre sistemas desordenados, campos aleatórios e a média sobre realizações da desordem para quantidades extensivas. A função zeta distribucional, um método alternativo ao truque do replica, é apresentada para demonstrar as contribuições para a massa quadrada renormalizada dadas por diagramas de um e dois laços nessa abordagem.

***Palavras-chave:*** desordem, quenched, euclideano, campos

# Contents

# Chapter 1

# Introduction

Disorder or randomness in a physical system can emerge from many different sources, and as a consequence, disordered systems have been extensively investigated for decades. Disorder systems have posed quite a challenge in both theoretical and experimental contexts. For example, in statistical mechanics [1, 2, 3, 4] and condensed matter physics [5]. The key point is to extend the understanding of criticality of clean systems to systems with inhomogeneities or impurities [6]. In statistical field theory, there are two types of disorder systems: annealed and quenched. Here, we are specifically interested in discussing quenched disorder systems. This type of disorder appears in many condensed matter systems, such as disordered metals, impure semiconductors, and classical or quantum spin systems [2, 3, 7, 8]. Unlike annealed disorder, treating quenched disorder requires evaluating the average of the logarithm of the partition function [9]. To address this problem, Edwards and Anderson proposed the *replica trick* [10]. Although the replica trick has been used in the literature for decades, a lack of mathematical rigor and the problem of interpreting the results from a physical standpoint have been persistent issues with this approach. As a result, alternative methods have been proposed [11, 12]. In this thesis, we employ an alternative method for averaging the disorder, proposed by Svaiter and Svaiter [13], known as the distributional zeta-function.

The aim of this work is to study the effects of quenched disorder on systems in the spontaneously symmetry-broken phase at low temperatures. Specifically, we investigate these effects on the two-loop contributions to the renormalized squared mass. Recent experimental and theoretical advances have generated increased interest in low-temperature physics and quantum phase transitions [14, 15, 16, 17, 18]. The intersection of these two research areas, quenched disorder and low temperatures [19, 20, 21, 22, 23], leads us to several questions, such as how models at ordered phase in low temperatures are affected by randomness.

Using the distributional zeta-function, we assume some probability distribution on the space of realizations of the disorder to discuss the effect of the disorder field in a Euclidean quantum scalar $\lambda\phi^4_{d+1}$ model at low temperatures in the broken symmetry phase. Criticality in these systems is induced by quantum and disorder fluctuations. In this case, the ground states of systems change in some fundamental way tuned by non-thermal control parameters [24, 25, 26, 27].

To discuss the effect of quantum fluctuations in a system with disorder in the symmetry-broken phase at low temperatures, we will use the imaginary-time formalism [28, 29, 30]. In this context, since the disorder is strongly correlated in imaginary time, the equivalence between a disorder Euclidean quantum $\lambda\phi^4_{d+1}$ model and a classical model defined on $\mathbb{R}^d \times \mathcal{S}^1$ will be used. For a pure system with this topology of space, the topological generation of mass has been discussed in the literature [31, 32, 33, 34, 35, 36, 37]. The study of the modified dynamics induced by the disorder, in this context, was made by Heymans et. al [38].

The structure of this work is as follows. In chapter 2, we start with a brief discussion about how to obtain the Euclidean propagator and the multi-loop expansion in the quantum field theory at finite temperature context. This is followed by the analytic regularization technique to evaluate the loop expansion. In sections 2.5 and 2.6, the renormalized thermal mass in the one-loop and two-loop approximation for the pure system in the broken symmetry phase is discussed. In chapter 3, we discuss the disorder systems and the averaging over the disorder realizations, followed by the *distributional zeta-function* method. In chapter 4, the effect of disorder on the renormalized squared mass in the one-loop and two-loop approximation, in the symmetry-broken phase, is discussed. The conclusions are given in chapter 5. We use the units $\hbar = c = k_B = 1$.

# Chapter 2

# The $\lambda\phi^4$ Euclidean quantum field theory

In this chapter, we will discuss some aspects of a scalar field at finite temperature in the imaginary time formalism [39]. In the first part, we will discuss the generating functionals and pertubative expansion of the two-point functions. Then, will be presented how to define the Euclidean propagators for a scalar field with a $\lambda\phi^4$ potential, incorporating the Matsubara frequencies. We will then proceed with the demonstration and evaluation of the loop contributions of the two-point Green functions within the context of the $\lambda\phi^4$ self-interaction with finite temperature.

## 2.1 Generating functional

In this section will be presented the discussion of generating functionals of Euclidean field theory. We begin with the functional representation of the Euclidean scalar field theory, defined in the Euclidean space $\mathbb{R}^{d+1}$, in the presence of a scalar source $J$ given by

$$Z[J] = \int [\mathrm{d}\phi] \exp\left[-\left(S(\phi) + \int \mathrm{d}^{d+1}x\ J(x)\phi(x)\right)\right]. \tag{2.1}$$

The $n$-point correlation function will be given by

$$\langle \phi(x)_1) \cdots \phi(x_n) \rangle_J = Z[J]^{-1} \prod_{i=1}^{n} \frac{\delta^n}{\delta J(x_i)} Z[J]. \tag{2.2}$$

When $J \to 0$ and in the symmetric phase, only correlations involving an even number of points do not vanish. They are translational invariant, and we will denote them by [40]

$$\begin{aligned}\langle \phi(x_1)\cdots\phi(x_n)\rangle &= Z[J]^{-1}\prod_{i=1}^{n}\frac{\delta^n}{\delta J(\mathbf{x}_i)}Z[J]\Big|_{J=0} \\ &= \int\prod_{1}^{n}\left(\frac{\mathrm{d}^{d+1}p_k}{(2\pi)^d}e^{-p_k\cdot x_k}\right)(2\pi)^{d+1}\delta\left(\sum p_k\right)G_n(p_1,\cdots,p_n).\end{aligned} \tag{2.3}$$

Where $G_n$ is the $n$-point Green function. The momentum conservation distribution $\delta\left(\sum p\right)$ has been extracted, so that in momentum space $G_n$ is defined on the linear manifold $\sum p = 0$. The *free energy*, $W = \ln Z[J]$, is the generating functional for the connected correlation functions, $G_c^{(n)}(\{x_n\})$. In the zero source limit,

$$G_c^{(n)}(\{x_n\}) = \langle \phi(x_1)\cdots\phi(x_n)\rangle_c = \prod_{i=1}^{n}\frac{\delta^n}{\delta J(x_i)}W[J]\Big|_{J=0}. \tag{2.4}$$

The meaning of this terminology comes from the fact that only connected diagrams appear in the perturbation expansion. From $W[J]$ its possible to obtain the generating

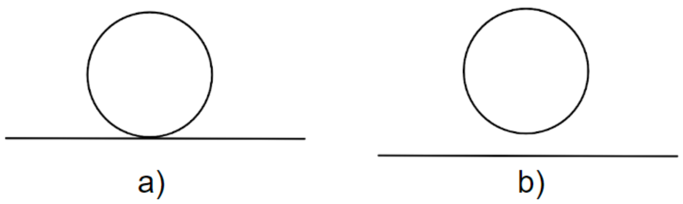


**Figure 2.1:** These are examples for the a) connected and b) disconnected diagrams. The connected one share a point with the line that represents the 2-points Green function (or the propagator) and the disconnected one do not share any point [40, 41, 42].

functional of *one particle irreducible* (1PI) Green functions, called in the literature as *vertex* functions, noted by $\mathit{\Gamma}[\phi]$, by applying a Legendre transformation. In the perturbation theory, the contributing diagrams cannot be disconnected by cutting an internal line, and propagators corresponding to the external lines are omitted. This is the origin of the qualification 1PI[1]. The quantity $\mathit{\Gamma}[\phi]$ is defined through

$$\mathit{\Gamma}[\phi] = \int \mathrm{d}^{d+1}x\ J(\mathbf{x})\phi(x) - W[J]. \tag{2.5}$$

[1] For a detailed discussion on one particle irreducible see [42].

Through the above expression, we can show that

$$\frac{\delta \Gamma[\phi]}{\delta \phi(x)} = J(x) \tag{2.6}$$

and

$$\frac{\delta W[J]}{\delta J(x)} = \phi(x) = \langle \phi(x) \rangle_J \,. \tag{2.7}$$

When $J$ tends to be uniform, the free energy appears as the integral of a constant density. The same is true for $\Gamma[\phi]$ when $\phi$ is uniforms, and we write in this case

$$\Gamma[\phi] = \int \mathrm{d}^{d+1}x \; V(\phi). \tag{2.8}$$

The effective potential $V(\phi)$, which takes into account the fluctuations, is a generalization of the corresponding term in the Lagrangian of the system.

Returning to the general case, the vertex functions are obtained by expanding $\Gamma[\phi]$ in increasing powers of $\phi$, as one does with $W[J]$ to get the connected functions. Through this procedure, it is possible to demonstrate that the second derivative of the vertex function is the functional inverse of the connected 2-point Green function [40, 42] and will be given as follows

$$\frac{\partial^2 \Gamma[\phi]}{\partial \phi^2} = G_c^{-1}(p), \tag{2.9}$$

where $G_c(p)$ is the Fourier transform of $G_c^{(2)}(x_1, x_2)$.

## 2.2 Multi-loop expansion

Here we will present the expansion to obtain the one- and two-loops. Considering the Euclidean $\lambda\phi^4$ theory, we began by expanding the generating functional $Z[J]$ around the bare coupling constant $\lambda$ as

$$\begin{aligned} Z[J] &= \int [\mathrm{d}\phi] \exp\left[ - \left( S + \int \mathrm{d}^{d+1}x \; J\phi \right) \right] \\ &= \sum_{n=0}^{\infty} \left( \int \mathrm{d}^{d+1}x \; V\left( \frac{\delta}{\delta J} \right) \right)^n \; Z_0[J], \end{aligned} \tag{2.10}$$

where $S$ is the action functional and $Z_0[J]$ is the Gaussian generation with an arbitrary source J. The last term of the above expression can be written as

$$Z_0[J] = N_0 \exp\left[ \frac{1}{2} \int \mathrm{d}^{d+1}x \int \mathrm{d}^{d+1}y \; J(x) G_0(x-y) J(y) \right] \tag{2.11}$$

where $N_0$ is the normalization factor, defined by $N_0 = \det^{1/2} G_0(\mathbf{x}-\mathbf{y})$, and $G_0$ is the free propagator. The unrenormalized perturbative series is obtained by expanding the first exponential and by performing, term by term, the differentiation operations. These implicitly contain Wick's theorem in the form

$$\begin{aligned}\langle \phi(x_1 \cdots x_{2n}\rangle_0 &= \prod_{i=1}^{2n} \frac{\delta^{2n}}{\delta J(x_i)} \frac{1}{2^n n!} (Z_0[J])^n \bigg|_{J=0} \\ &= \sum_{\text{distinct terms}} G_0(x_{a_1} - x_{a_2}) \cdots G_0(x_{a_{2n-1}} - x_{a_{2n}}).\end{aligned} \tag{2.12}$$

It is convenient to express the perturbative rules directly in momentum space for the vertex functions. To each term of the expansion of $Z[J]$ is associated a representative diagram combining vertices and lines. Only the irreducible diagram are considered in the calculation of $\Gamma_n$. For the $\phi^4$ interaction, each vertex is associated with a factor $-\lambda$ and a momentum conservation $\delta$-function, $(2\pi)^{d+1}\delta(\Sigma_p)$, for the sum $\Sigma_p$ of internal and external momenta entering the vertex. In this thesis we will restrict the case for the 2-point vertex functions. The first terms of the vertex function will the terms associated to $O(\lambda^0)$, $O(\lambda^1)$ and $O(\lambda^2)$. The terms associated to order 1 and 2 of $\lambda$ are called in the literature one- and two-loops, their diagram representation can be see in fig. 2.2.

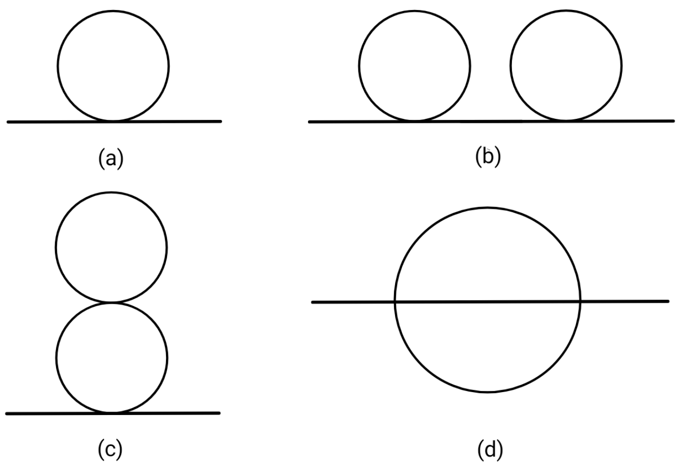


**Figure 2.2:** The first diagram, (a), represents the 1-loop diagram and is commonly referred to as the *tadpole* diagram. The remaining three diagrams correspond to the 2-loop diagrams. The first 2-loop diagram, (b), is a 1PR (one-particle reducible) diagram, while the other two, (c) and (d), are 1PI (one-particle irreducible) diagrams. These last two diagrams are known as the *double scoop* and *sunset* diagrams, respectively.

In the following we will present the one- and two-loops contributions of the vertex function.

The one-loop contribution is the *tadpole* diagram represented by Figure 2.2-a and given by

$$T_1 = -\frac{\lambda}{2}\int \frac{\mathrm{d}^{d+1}k}{(2\pi)^{d+1}}\varDelta\left(k\right), \tag{2.13}$$

where $\varDelta(p)$ is the propagator.

The two-loop diagrams consist of three different diagrams. The first one, represented by Figure 2.2-b, will be called the *double tadpole* diagram. The double tadpole diagram is a *one-particle reducible* (1PR) diagram. Therefore, we can split this diagram into two parts, each with an $f$-factor, as follows

$$T_2 = f_{T_2}(\lambda)\int \frac{\mathrm{d}^{d+1}k}{(2\pi)^{d+1}}\varDelta\left(k\right), \tag{2.14}$$

$$T_3 = f_{T_3}(\lambda)\int \frac{\mathrm{d}^{d+1}l}{(2\pi)^{d+1}}\varDelta\left(l\right). \tag{2.15}$$

This diagram can be treated as a one-loop diagram.

The next two-loop contribution is called the *double scoop* diagram, represented by Figure 2.2-c. This diagram is *one-particle irreducible* (1PI), so we cannot split it like the double tadpole. The diagram is given by

$$D = f_D(\lambda)\int \frac{\mathrm{d}^{d+1}k}{(2\pi)^{d+1}}\int \frac{\mathrm{d}^{d+1}l}{(2\pi)^{d+1}}\varDelta\left(k\right)\left[\varDelta\left(l\right)\right]^2. \tag{2.16}$$

This diagram can also be written as $D = f\ T_1(\partial/\partial m_0^2)T_1$.

The last two-loop contribution is a non-trivial diagram known as the *sunset* diagram, represented by Figure 2.2-d. Similar to the previous diagram, this is a 1PI diagram. As we can see in the representation, the third momentum can be written as the external momentum, P, minus the other momenta. Therefore, the sunset diagram is given by

$$\varSigma = f_\varSigma(\lambda)\int \frac{\mathrm{d}^{d+1}k}{(2\pi)^{d+1}}\int \frac{\mathrm{d}^{d+1}l}{(2\pi)^{d+1}}\frac{\varDelta\left(k\right)\varDelta\left(l\right)}{\left[\varDelta\left(P-k-l\right)\right]^{-1}} \tag{2.17}$$

In further sections we will consider the thermal versions of these diagrams. The differences between the non-thermal and thermal will presented in the next sections.

## 2.3 The Euclidean propagator

We begin with the action functional for a Euclidean quantum scalar field at finite temperature, defined in the space $\mathbb{R}^d \times \mathcal{S}^1$, given by

$$S_\beta(\phi) = \int_0^\beta \mathrm{d}\tau \int \mathrm{d}^d x \left[\phi(\tau,\mathbf{x}) \left(-\frac{\partial^2}{\partial\tau^2} - \Delta + \mu_0^2\right) \phi(\tau,\mathbf{x}) + V(\phi)\right], \tag{2.18}$$

where $\Delta$ is the Laplacian in $\mathbb{R}^d$, $\phi(\tau,\mathbf{x})$ is a real field, $\mu_0$ is a parameter with mass dimension, and the self-interaction is contained in $V(\phi)$. The generating functional of correlation functions is defined as

$$Z_\beta[J] = N_\beta \int_{\mathcal{C}} [\mathrm{d}\phi] \exp\left[-\left(S_\beta(\phi) + \int_0^\beta \mathrm{d}\tau \int \mathrm{d}^d x\ J(\tau,\mathbf{x})\phi(\tau,\mathbf{x})\right)\right], \tag{2.19}$$

where $[\mathrm{d}\phi]$ represents a functional measure, given by $[\mathrm{d}\phi] = \prod_{\tau,\mathbf{x}} \mathrm{d}\phi(\tau,\mathbf{x})$, and $\mathcal{C}$ denotes the path defined by the periodic condition $\phi(\mathbf{x},\tau) = \phi(\mathbf{x},\tau+\beta)$, and $N_\beta$ is a normalization factor. From now on, the subscript $\beta$, on the functional and action, will be omitted for simplification purpose. The $n$-point correlation functions of the model are given by

$$\langle\phi(\tau_1,\mathbf{x}_1)\cdots\phi(\tau_n,\mathbf{x}_n)\rangle = \frac{1}{Z}\int [\mathrm{d}\phi] \prod_{i=1}^{n} \phi(\tau_i,\mathbf{x}_i) \exp\left[-S(\phi)\right]. \tag{2.20}$$

where $Z$ is the partition function for a non-interacting scalar field with source $J=0$. From the generating functional of correlation functions (2.19), we can define the generating functional of connected functions $W[J]$. By applying the periodic condition on $S(\phi)$, we can rewrite (2.19) as

$$Z[J] = N e^{-\langle V(\frac{\delta}{\delta J})\rangle_\beta} \exp\left[\frac{1}{2}\left\langle J(\tau_x,\mathbf{x})\Delta_\beta(\tau_x-\tau_y,\mathbf{x}-\mathbf{y})J(\tau_y,\mathbf{y})\right\rangle_\beta\right], \tag{2.21}$$

where $\langle\cdots\rangle_\beta$ means the integration over $x$ and $\tau$ in the imaginary-time interval $[0,\beta]$. The Euclidean propagator, $\Delta_\beta(\tau,\mathbf{x})$, satisfies the following expression

$$\left(-\frac{\partial^2}{\partial\tau^2} - \Delta + \mu_0^2\right) \Delta_\beta(\tau_x-\tau_y,\mathbf{x}-\mathbf{y}) = \delta(\tau_x-\tau_y)\delta^d(x-y). \tag{2.22}$$

Let us write the Fourier transform in the space coordinate of $\Delta_\beta$ as

$$\Delta_\beta(\tau_x-\tau_y,\mathbf{x}-\mathbf{y}) = \int \frac{\mathrm{d}^d k}{(2\pi)^d} e^{i\mathbf{k}\cdot(\mathbf{x}-\mathbf{y})} \Delta_\beta(\tau_x-\tau_y,\mathbf{k}), \tag{2.23}$$

if we apply (2.23) to (2.22), it is possible to verify that $\Delta_\beta(\tau_x-\tau_y,\mathbf{k})$ satisfies the differential equation

$$\left(-\frac{\partial^2}{\partial\tau^2} + \mathbf{k}^2 + m_0^2\right) \Delta_\beta(\tau_x-\tau_y,k) = \delta(\tau_x-\tau_y). \tag{2.24}$$

To write the Fourier transform of the Euclidean propagator, we need to write the Fourier transform in imaginary time as, with $\tau \in [0, \beta]$,

$$\Delta_\beta(\tau, \mathbf{x}) = \frac{1}{\beta} \sum_{n \in \mathbb{Z}} e^{-i\omega_n \tau} \Delta_\beta(\omega_n, \mathbf{k}), \tag{2.25}$$

and the inverse transform defined as

$$\Delta_\beta(\omega_n, \mathbf{k}) = \int_0^\beta \mathrm{d}\tau e^{i\omega_n \tau} \Delta_\beta(\tau, \mathbf{x}). \tag{2.26}$$

Substituting (2.25) in (2.23) we have that

$$\Delta_\beta(\tau_x - \tau_y, \mathbf{x} - \mathbf{y}) = \frac{1}{\beta} \sum_{n \in \mathbb{Z}} \int \frac{\mathrm{d}^3 k}{(2\pi)^3} e^{-i(\omega_n \tau - \mathbf{k} \cdot \mathbf{x})} \Delta_\beta(\omega_n, \mathbf{k}), \tag{2.27}$$

then, the Fourier transform of the Euclidean propagator is given by

$$\Delta_\beta(\omega_n, \mathbf{k}) = \frac{1}{\omega_n^2 + \omega_k^2}. \tag{2.28}$$

The $\omega_k$ is the natural frequency, defined by $\omega_k^2 = \mathbf{k}^2 + \mu_0^2$, and $\omega_n$ are the Matsubara frequencies. For the scalar field, $\omega_n = \frac{2\pi n}{\beta}$, and for Dirac fields, $\omega_n = \frac{\pi(2n+1)}{\beta}$.

## 2.4 Spontaneously broken symmetry

In this section, we discuss the spontaneously broken symmetry phase of the $\lambda\phi^4$ theory. We will examine the contributions to the renormalized squared mass in this scenario. Let us begin by writing the action functional, where we replace $\mu^2$ with $-\mu^2$ to account for the spontaneous symmetry breaking,

$$S(\phi) = \int_0^\beta \mathrm{d}\tau \int \mathrm{d}^d x \left[ \phi(\tau, \mathbf{x}) \left( -\frac{\partial^2}{\partial \tau^2} - \Delta - \mu_0^2 \right) \phi(\tau, \mathbf{x}) + \frac{\lambda}{4!} \phi^4(\tau, \mathbf{x}) \right] \tag{2.29}$$

This action possesses the discrete symmetry $\phi \to \phi' = -\phi$. However, when $\mu^2 > 0$, this symmetry is spontaneously broken by the vacuum, leading to the development of a non-zero expectation value for $\phi$. We denote this expectation value as $\langle 0 | \phi | 0 \rangle = v$, where $v$ is

$$v = \left( \frac{\mu^2}{\lambda} \right)^{\frac{1}{2}}. \tag{2.30}$$

Perturbing around this vacuum, we can define a shifted field

$$\phi' = \phi - v. \tag{2.31}$$

In terms of this field, we have the following potential

$$V(\phi) = \mu^2\phi^2 + \lambda v\phi^3 + \frac{\lambda}{4}\phi^4 \tag{2.32}$$

In this new theory, the effective mass squared will be given by

$$m_0^2 = 3\lambda v^2 - \mu^2. \tag{2.33}$$

This new theory leads us to rewrite the correction to the squared mass in the one-loop approximation

$$m_R^2 = -\mu^2 + \delta\mu^2 + \varDelta m^2(\beta) \tag{2.34}$$

as

$$m_R^2(\beta,\mu) = m_0^2 + \delta m_0^2 + f_1\varDelta m_1^2(\beta,\mu) + f_2\varDelta m_2(\beta,\mu). \tag{2.35}$$

In the above expression, $\delta m_0^2$ represents the counterterm arising from the renormalization procedure. The factors $f_1$ and $f_2$ are the symmetry factors associated with the mass contributions. The terms $\varDelta m$ correspond to the contributions from the one-loop diagrams. In this case, due to the shift from the spontaneously broken symmetry, the one-loop contributions arise from the tadpole and the bubble diagram (fig. 2.3).

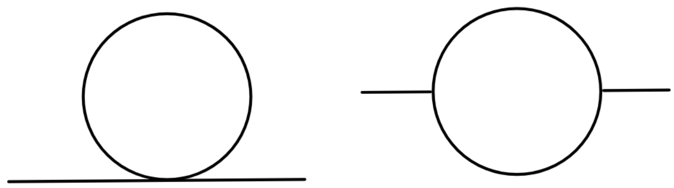

**Figure 2.3:** The first diagram is the Tadpole diagram, and the second diagram is the self-energy diagram, often referred to as the *Bubble diagram*. The Bubble diagram arises from the shift in the spontaneously broken symmetry scenario.

## 2.5 Evaluation of one-loop diagram

In this section, we will discuss the analytic regularization of the one-loop approximation and present its contribution to the renormalized squared mass. We start by considering the mass correction defined by the following expression

$$\varDelta m_s^2(\beta,\mu) = \frac{F(\lambda,\mu,s)}{\beta}\sum_{n\in\mathbb{Z}}\int\frac{\mathrm{d}^d p}{(2\pi)^d}\frac{1}{(\mathbf{p}^2 + m_0^2 + \omega_n^2)^s}, \tag{2.36}$$

where $\omega_n = \frac{2\pi n}{\beta}$ and $F(\lambda, \mu, s)$ represents an arbitrary coupling constant associated with each correction. The equation can be rearranged as follows

$$\Delta m_s^2(\beta,\mu) = \frac{F(\lambda,\mu,s)\beta}{2^{d+1}\pi^{\frac{d}{2}+1}\Gamma\left(\frac{d}{2}\right)} \int_0^\infty \mathrm{d}p\ p^{d-1} \sum_{n\in\mathbb{Z}} \left(\pi n^2 + \frac{\beta^2}{4\pi}\left(p^2+m_0^2\right)\right)^{-s} \tag{2.37}$$

and this function is defined in the region where the above integral converges, specifically for $Re(s) > s_0$. To further analyze this expression, we can perform a Mellin transform [43, 44], which is defined by

$$\frac{1}{(P^2+\alpha)^s} = \frac{1}{\Gamma(s)} \int_0^\infty \mathrm{d}t\ t^{s-1} \exp\left[-(P^2+\alpha)t\right], \tag{2.38}$$

the mass correction can be rewritten as

$$\Delta m_s^2(\beta,\mu) = \frac{F(\lambda,\mu,s)\beta}{2^{d+1}\pi^{\frac{d}{2}+1}\Gamma\left(\frac{d}{2}\right)\Gamma\left(s\right)} \sum_{n\in\mathbb{Z}} \int_0^\infty \mathrm{d}p\, p^{d-1} \int_0^\infty \mathrm{d}t\, t^{s-1} \exp\left[-\left(\pi n^2 + \frac{\beta^2}{4\pi}\left(p^2+m_0^2\right)\right)t\right]. \tag{2.39}$$

Let us define the dimensionless quantity $r^2 = \frac{\beta^2 p^2}{4\pi}$. After this variable change, the following function is obtained

$$\Delta m_s^2(\beta,\mu) = \frac{F(\lambda,\mu,s)\beta^{1-d}}{2\pi\Gamma\left(\frac{d}{2}\right)\Gamma\left(s\right)} \sum_{n\in\mathbb{Z}} \int_0^\infty \mathrm{d}r\ r^{d-1} \int_0^\infty \mathrm{d}t\ t^{s-1} \exp\left[-\left(\pi n^2 + r^2 + \frac{\beta^2}{4\pi}m_0^2\right)t\right]. \tag{2.40}$$

After performing the $r$ integral, the result will be

$$\Delta m_s^2(\beta,\mu) = F_d(\lambda,\beta,\mu,s) \int_0^\infty \mathrm{d}t\ t^{s-\frac{d}{2}-1} \exp\left[-\frac{m_0^2\beta^2}{4\pi}t\right] \Theta(t), \tag{2.41}$$

with

$$F_d(\lambda,\beta,\mu,s) = \frac{F(\lambda,\mu,s)}{2\pi\Gamma\left(s\right)} \left(\frac{1}{\beta}\right)^{d-1} \tag{2.42}$$

and $\Theta(t)$ being the Jacobi $\Theta$-function, given by

$$\Theta(\nu) = \sum_{n\in\mathbb{Z}} \exp\left[-\pi n^2 \nu\right]. \tag{2.43}$$

We can split (2.41) into two parts by considering the $t$-integral over the intervals $[0,1]$ and $[1,\infty]$. By utilizing the symmetry of the $\Theta$-function, we can rewrite the interval $[0,1]$ as $[1,\infty]$. After these modifications, we obtain

$$\Delta m_{s,1}^2(\beta,\mu) = \frac{F_d(\lambda,\beta,\mu,s)}{2} \int_1^\infty \mathrm{d}t\ t^{s+\frac{d}{2}-\frac{1}{2}} \exp\left[-\frac{m_0^2\beta^2}{4\pi t}\right] \Theta(t) \tag{2.44}$$

and

$$\varDelta m_{s,2}^2(\beta,\mu) = \frac{F_d(\lambda,\beta,\mu,s)}{2}\int_1^\infty \mathrm{d}t\ t^{s-\frac{d}{2}-1}\exp\left[-\frac{m_0^2\beta^2}{4\pi}t\right]\varTheta(t). \tag{2.45}$$

From the definition of the $\psi$-function, $\psi(\nu) = \sum_{n=1}^\infty \exp\left[-\pi n^2\nu\right]$ and $\psi(\nu) = \frac{1}{2}(\varTheta(\nu) - 1)$, we can rewrite $\varDelta m_s^2(\beta,\mu)$ as having four contributions. Therefore, these contributions are given by

$$I_d^{(1)}(\beta,s) = 2\int_1^\infty \mathrm{d}t\ t^{s-\frac{d}{2}-1}\exp\left[-\frac{m_0^2\beta^2}{4\pi}t\right]\psi(t), \tag{2.46}$$

$$I_d^{(2)}(\beta,s) = 2\int_1^\infty \mathrm{d}t\ t^{s+\frac{d}{2}-\frac{1}{2}}\exp\left[-\frac{m_0^2\beta^2}{4\pi t}\right]\psi(t), \tag{2.47}$$

$$I_d^{(3)}(\beta,s) = \int_1^\infty \mathrm{d}t\ t^{s-\frac{d}{2}-1}\exp\left[-\frac{m_0^2\beta^2}{4\pi}t\right], \tag{2.48}$$

$$I_d^{(4)}(\beta,s) = \int_1^\infty \mathrm{d}t\ t^{s+\frac{d}{2}-\frac{1}{2}}\exp\left[-\frac{m_0^2\beta^2}{4\pi t}\right]. \tag{2.49}$$

With the above functions, our mass correction will be given by

$$\varDelta m_s^2(\beta,\mu) = \frac{F_d(\lambda,\beta,\mu,s)}{2}\sum_{k=1}^{4} I_d^{(k)}(\beta,s). \tag{2.50}$$

From this function, we can obtain the result for the *tadpole* and *bubble* diagrams by setting $s = 1$ and $s = 2$, respectively. For further discussion about these diagrams, see [37, 38].

## 2.6 Two-loops diagram evaluation

In this section, we will present the thermal corrections for the two-loop approximation in the context given in the previous section. The two-loop contributions to the renormalized squared mass correction are given by

$$m_R^2(\beta,\mu) = m_0^2 + \delta m_0^2 + f_{(2)}\varDelta m_{(2)}^2(\beta,\mu) + f_{(3)}\varDelta m_{(3)}^2(\beta,\mu). \tag{2.51}$$

where $m_0^2$ is the bare squared mass, $\delta m_0^2$ is the counterterm from the renormalization procedure, $f_{(2)}$ and $f_{(3)}$ are the immaterial symmetry factors for the two-loop contributions, and $\varDelta m_{(2)}^2(\beta,\mu)$ and $\varDelta m_{(3)}^2(\beta,\mu)$ are the mass corrections from the double scoop and sunset diagrams, respectively.

Although the double tadpole diagram is a two-loop diagram, it does not contribute to the mass correction. However, it will have the same result as the one-loop diagram. We will evaluate all two-loop diagrams, including the double tadpole. Let us evaluate each two-loop diagram independently.

### 2.6.1 *Double-Tadpole*

Our first task is to evaluate the *double tadpole* diagram, represented by figure 2.2-b. To do this, we will separate the diagram into two branches by cutting the external leg between both loops. Let us perform the calculation of (2.14 - 2.21). After the Mellin transform and momentum integration, the mass correction of this diagram will have the following form

$$\Delta m^2_{(1),(\frac{1}{2})}(\beta,\mu) = F_{(\frac{1}{2})} \sum_{n\in\mathbb{Z}} \int_0^\infty \mathrm{d}t\, t^{\frac{d}{2}} \exp\left[-\frac{m_0^2\beta^2 t}{4\pi}\right] \exp\left[-\pi n^2 t\right], \tag{2.52}$$

here, the second subscript represents the first and second branch of the diagram. It is easy to see that the above function is the same as (2.41) with $s = 1$, as expected. For the calculation of the $F$-factor for each branch, we have that [45, 46]

$$\begin{aligned} m^2 &= m_R^2 \left[1 + \sum_{\nu=1}^{\infty}\sum_{\eta=1}^{\infty} \frac{b_{\nu\eta}\lambda_R^\eta}{(n-4)^\nu}\right], \\ \lambda &= \mu^{4-n}\left[\lambda_R + \sum_{\nu=1}^{\infty}\sum_{\eta=1}^{\infty} \frac{a_{\nu\eta}\lambda_R^\eta}{(n-4)^\nu}\right]. \end{aligned} \tag{2.53}$$

As a trivial diagram, the result of this loop will be the same as discussed before, for the one-loop. We can verify that each part of this diagram will have the result (2.50) for $s = 1$,

$$\Delta m^2_{(1),1}(\beta,\mu) = F_1(\lambda,\beta,\mu) \sum_{k=1}^{4} I_d^k(\beta,1), \tag{2.54}$$

$$\Delta m^2_{(1),2}(\beta,\mu) = F_2(\lambda,\beta,\mu) \sum_{k=1}^{4} I_d^k(\beta,1) \tag{2.55}$$

and the $F$-factor as

$$F_1(\lambda,\beta,\mu) = -\frac{3\lambda_R^2}{2(4\pi)^3}\frac{(\mu^2)^{4-d}}{4-d}\beta^{1-d}, \tag{2.56}$$

$$F_2(\lambda,\beta,\mu) = -\frac{\lambda_R^2 m_R^2}{2(4\pi)^3}\frac{(\mu^2)^{4-d}}{4-d}\beta^{1-d}. \tag{2.57}$$

### 2.6.2 *Double Scoop*

The next diagram to be evaluated is the *double scoop*. This diagram is defined as (2.16). As we can see, the momenta in this diagram are not connected. However, we can work on each momentum integral independently. Let us repeat it here for practical purposes

$$\Delta m^2_{(2)}(\beta,\mu) = \frac{(-\lambda_R)^2(\mu^2)^{4-d}}{4\beta^2} \sum_{n,r\in\mathbb{Z}} \int \frac{\mathrm{d}^d k}{(2\pi)^d} \int \frac{\mathrm{d}^d l}{(2\pi)^d} \Delta_\beta\left(\omega_n, \mathbf{k}\right) \left[\Delta_\beta\left(\omega_r, \mathbf{l}\right)\right]^2. \tag{2.58}$$

Now we can begin by transforming both integrals as follows

$$\frac{1}{\beta}\int_{-\infty}^{\infty} \frac{\mathrm{d}^d k}{(2\pi)^d} \frac{1}{(k^2+m_0^2+\omega_n^2)} \equiv \frac{\beta}{2^{d+1}\pi^{\frac{d}{2}+1}\Gamma\left(\frac{d}{2}\right)} \int_0^{\infty} \mathrm{d}k\; k^{d-1} \left(\pi n^2 + \frac{\beta^2}{4\pi}\left(\mathbf{k}^2+m_0^2\right)\right)^{-1}, \tag{2.59}$$

and

$$\frac{1}{\beta}\int_{-\infty}^{\infty} \frac{\mathrm{d}^d l}{(2\pi)^d} \frac{1}{(k^2+m_0^2+\omega_r^2)} \equiv \frac{\beta}{2^{d+1}\pi^{\frac{d}{2}+1}\Gamma\left(\frac{d}{2}\right)} \int_0^{\infty} \mathrm{d}l\; l^{d-1} \left(\pi r^2 + \frac{\beta^2}{4\pi}\left(\mathbf{l}^2+m_0^2\right)\right)^{-2}. \tag{2.60}$$

Here, in both integrals, we can define dimensionless variables as $K^2 = \frac{\beta^2 k^2}{4\pi}$ and $L^2 = \frac{\beta^2 l^2}{4\pi}$. By repeating the Mellin transform procedure, the integrals can be rewritten as follows

$$k\text{-integral} = \frac{\beta^{1-d}}{2\pi\Gamma\left(\frac{d}{2}\right)} \sum_{n\in\mathbb{Z}} \int_0^{\infty} \mathrm{d}K\; K^{d-1} \int_0^{\infty} \mathrm{d}t_1 \exp\left[-\left(\pi n^2 + K^2 + \frac{\beta^2}{4\pi}m_0^2\right)t_1\right], \tag{2.61}$$

$$l\text{-integral} = \frac{\beta^{1-d}}{2\pi\Gamma\left(\frac{d}{2}\right)} \sum_{r\in\mathbb{Z}} \int_0^{\infty} \mathrm{d}L\; L^{d-1} \int_0^{\infty} \mathrm{d}t_2\; t_2 \exp\left[-\left(\pi r^2 + L^2 + \frac{\beta^2}{4\pi}m_0^2\right)t_2\right]. \tag{2.62}$$

As we can see, after performing both integrations, we will obtain the same result as (2.41) for $s$ equal to 1 and 2, as expected. These integrals can be written as

$$k\text{-integral} = \frac{\beta^{1-d}}{2\pi} \int_0^{\infty} \mathrm{d}t_1 t_1^{-\frac{d}{2}} \exp\left[-\frac{\beta^2}{4\pi}m_0^2 t_1\right] \Theta(t_1), \tag{2.63}$$

$$l\text{-integral} = \frac{\beta^{1-d}}{2\pi} \int_0^{\infty} \mathrm{d}t_2\; t_2^{1-\frac{d}{2}} \exp\left[-\frac{\beta^2}{4\pi}m_0^2 t_2\right] \Theta(t_2). \tag{2.64}$$

The result, after all the procedures described in the previous section, will be

$$\Delta m^2_{(2)}(\beta,\mu) = \frac{\lambda_R^2}{(4\pi)^2}\frac{(\mu^2)^{4-d}}{(\beta^2)^{d-1}} \left(\sum_{k=1}^{4} I_d^{(k)}(\beta,1)\right)\left(\sum_{l=1}^{4} I_d^{(l)}(\beta,2)\right) \tag{2.65}$$

### 2.6.3 *Sunset*

The only non-trivial diagram, and the last of the two-loop contributions to be evaluated, is the *sunset* diagram, which was previously commented on and defined by (2.17). This diagram is more challenging to evaluate due to the connected momenta and frequencies. Let us start by writing the diagram, with the Mellin transform already performed, as follows

$$\begin{aligned}\mathit{\Delta} m^2_{(3)}(\beta,\mu) =&\frac{\lambda_R^2(\mu^2)^{4-d}}{\beta^2}\sum_{n,r\in\mathbb{Z}}\int_0^\infty\frac{\mathrm{d}^dk}{(2\pi)^d}\int_0^\infty\frac{\mathrm{d}^dl}{(2\pi)^d}\int_0^\infty[\mathrm{d}X]\exp\left\{-x\left[\frac{\beta^2}{4\pi}\left(\mathbf{k}^2+m_0^2\right)+\pi n^2\right]\right.\\&\left.-y\left[\frac{\beta^2}{4\pi}\left(\mathbf{l}^2+m_0^2\right)+\pi r^2\right]-z\left[\frac{\beta^2}{4\pi}\left((\mathbf{p}-\mathbf{k}-\mathbf{l})^2+m_0^2\right)+\pi(t-n-r)^2\right]\right\},\end{aligned} \tag{2.66}$$

where $[\mathrm{d}X]=\mathrm{d}x\mathrm{d}y\mathrm{d}z$. Now the momenta integrations will be performed, and after some rearrangements, the obtained result will be

$$\begin{aligned}\mathit{\Delta} m^2_{(3)}(\beta,\mu) =&\frac{\lambda_R^2(\mu^2)^{4-d}}{4^{d-1}\beta^{2d}}\sum_{n,r\in\mathbb{Z}}\int_0^\infty[\mathrm{d}X]\,c^{\frac{1-d}{2}}\exp\left[-\pi\left(\frac{\beta^2}{4\pi^2}m_0^2(x+y+z)+\frac{\beta^2}{4\pi^2}\mathbf{p}^2\frac{xyz}{c}\right)\right]\\&\times\exp\left[-\pi\left(n^2x+r^2y+(t-n-r)^2z\right)\right]\end{aligned} \tag{2.67}$$

with $c=xy+xz+yz$. To continue the evaluation, we need to rearrange the frequency part. To do this, a *Poisson summation* can be performed, and the desired form will be achieved as

$$\begin{aligned}\mathit{\Delta} m^2_{(3)}(\beta,\mu) =&\frac{\lambda_R^2(\mu^2)^{4-d}}{(4\beta^2)^d}\sum_{n,r\in\mathbb{Z}}\int_0^\infty[\mathrm{d}X]\,c^{-\frac{d}{2}}\exp\left[-\pi\left(\frac{\beta^2}{4\pi^2}m_0^2(x+y+z)+\frac{\beta^2}{4\pi^2}p^2\frac{xyz}{c}\right)\right]\\&\times\exp\left[-\frac{\pi}{c}\left(n^2(y+z)+r^2(x+z)-2rnz\right)-i\beta p_0z\frac{(ny+rx)}{c}\right],\end{aligned} \tag{2.68}$$

here we perform some rearrangements by defining $p=(\mathbf{p},p_0)$ and $t=\frac{\beta}{2\pi}p_0$. Now we can split the above function for $n,r=0$ and $n,r\neq 0$. For the $n,r=0$ we have that

$$\mathit{\Delta} m^2_{(3)}(\beta,\mu)|_{n,r=0}=\frac{\lambda_R^2(\mu^2)^{4-d}}{(4\beta^2)^d}\int_0^\infty[\mathrm{d}X]\,c^{-\frac{d}{2}}\exp\left[-\pi\left(\frac{\beta^2}{4\pi^2}m_0^2(x+y+z)+\frac{\beta^2}{4\pi^2}p^2\frac{xyz}{c}\right)\right]. \tag{2.69}$$

For $n, r \neq 0$ we can show that

$$\Delta m^2_{(3)}(\beta,\mu)|_{n,r\neq 0} = \frac{\lambda_R^2(\mu^2)^{4-d}}{(4\beta^2)^d}\int_0^\infty [\mathrm{d}X]\, c^{-\frac{d}{2}} \exp\left[-\pi\left(\frac{\beta^2}{4\pi^2}m_0^2(x+y+z)+\frac{\beta^2}{4\pi^2}p^2\frac{xyz}{c}\right)\right] \times \left[\sum_{n,r=0}^{\infty} e^{-\frac{\pi}{c}\left[n^2(y+z)+r^2(x+z)-2rnz\right]-i\beta p_0 z\frac{(ny+rx)}{c}} - 1\right], \tag{2.70}$$

As the only other possible divergence emerges from the case $n \neq 0$,$r = 0$ or $n = 0$,$r \neq 0$, we can set $r = 0$ and obtain

$$\Delta m^2_{(3)}(\beta,\mu)|_{n\neq 0,r=0} = \frac{\lambda_R^2(\mu^2)^{4-d}}{(4\beta^2)^d}\int_0^\infty [\mathrm{d}X]\, c^{-\frac{d}{2}} \exp\left[-\pi\left(\frac{\beta^2}{4\pi^2}m_0^2(x+y+z)+\frac{\beta^2}{4\pi^2}p^2\frac{xyz}{c}\right)\right] \times\left[\Theta\left(\frac{-\beta p_0 zy}{2c}\middle|\frac{y+z}{c}\right)-1\right], \tag{2.71}$$

The case $r \neq 0$ can be achieved by setting $n = 0$ in (2.70). In this case, we obtain the same function with $y \to x$ in the $\theta$-function. The evaluation of these diagrams in the pure system has already been done in the literature, where they are separated into non-thermal and thermal contributions [37].

# Chapter 3

# Disordered systems

Statistical mechanics has been successful in describing the macroscopic properties of many condensed matter systems, such as phase transitions and ordered states, by assuming translational invariance as idealized homogeneous systems. However, real systems often exhibit inhomogeneities and impurities that break, for example, translational invariance [6].

In this section, we will discuss some generalities of the types of disorder, with a particular focus on quenched disorder. We will also introduce some aspects of glassy systems and random fields. While we will briefly mention the replica trick, the main emphasis will be on the discussion of the distributional zeta-function method, which is the primary method used in this study.

## 3.1 Types of disorder in physical systems

Disorder or randomness in a physical system can arise from various sources, including impurity atoms, vacancies in a crystal, dislocations, or grain boundaries in a crystal lattice, among others. In the study of disorder systems, two types of disorder are commonly distinguished: annealed disorder and quenched disorder.

### 3.1.1 Annealed disorder

In systems with annealed disorder, the fluctuations of the degrees of freedom associated with impurities occur on a timescale much smaller than the measurement time of the system. As a result, the disorder is in thermal equilibrium with other degrees of freedom in the system. This puts the disorder and non-disorder variables on equal footing. To study such systems, it is necessary to compute the partition function by summing over all configurations of the original components that describe the pure system and the impurities.

To illustrate this, let us consider an example. Suppose we have a pure piece of ferromagnetic material that is heated to its melting temperature and then slowly cooled to crystallize while adding some impurities. In this case, the impurities will be in thermal equilibrium with the degrees of freedom of the original components of the pure system. The Gibbs distribution can be used to model the impurities [47, 48]. In general, the partition function $Z$ of the system can be written as

$$Z = \mathrm{Tr}_{(h,s)} e^{-\beta H(h,s)}, \tag{3.1}$$

where $h$ and $s$ represent the impurity and system degrees of freedom, respectively. $H$ is the Hamiltonian of the system, and $\beta$ is the inverse temperature. The disorder variables being in thermal equilibrium with the system degrees of freedom allows us to treat them in the same manner. This simplifies the study of annealed disorder systems significantly. Now, the free energy can be rewritten as follows

$$F = -\frac{1}{\beta V} \ln Z. \tag{3.2}$$

As we can see, the thermodynamic properties of this class of systems are obtained from the partition function, which is traced over the disorder in the same way that we trace over the thermal variables. Although annealed disorder has considerable effects on systems in which it appears, examples can be found in references such as [49, 50, 51, 52, 53].

### 3.1.2 Quenched disorder

In contrast to annealed disorder, the degrees of freedom associated with impurities in systems with quenched disorder evolve on a different time scale compared to those characterizing the "clean" system. Their fluctuations are much slower, giving them the property of being fixed or "frozen" relative to the other degrees of freedom. In other words, quenched disorder is static. Almost all disorder in condensed matter systems falls into this category. In the experimental context, the time scale of the measurement is much smaller than the dynamical time scale of the impurities, which implies that if we take multiple samples, the corresponding disordered variables assume well-defined time-independent vale. In this context, each realization of the disorder corresponds to a unique realization of the random variables, while their distribution describes the fluctuations between different realizations.

Due to the nature of quenched randomness, in contrast to annealed disorder, the degrees of freedom associated with impurities in the system are not in thermal equilibrium with the other degrees of freedom. This means that each disorder configuration of the system will be unique. Since this type of disorder is static and the impurities are not allowed to move, the network structure remains fixed and the interactions are established. Therefore, to study the thermodynamic properties of the system, the partition function is determined for a specific disorder realization, and only the equilibrium quantities are averaged over different distributions of the impurities. In this context, the partition function is given by

$$Z(h) = \mathrm{Tr}_{(s)} e^{-\beta H(h,s)}. \tag{3.4}$$

The partition function will depend on all the impurity variables $h$, and as a result, the calculation of thermodynamic quantities for the system becomes more challenging compared to the annealed case. Since the thermal averages are not equivalent to averages over the disorder, it is important to differentiate between the characteristics of the dynamical degrees of freedom and the disordered variables when defining the thermodynamic properties of a system. Ideally, we would like to calculate quantities that determine the equilibrium of the system by computing averages over the Boltzmann measure. However, due to the disorder, we can only evaluate quantities that are averaged over both the thermal distribution and the disorder distribution.

## 3.2 Average over the disorder

In disorder systems, the outcomes of a sequence of experiments on a given observable can vary from one sample to another. In these systems, certain quantities, particularly extensive quantities like the free energy, exhibit the property of being "self-averaging" in the thermodynamic limit [54]. This means that they take the same value for each realization of the disorder that has a non-zero probability. In other words, as the volume of the system approaches infinity, the fluctuations between different samples diminish, and the average value coincides with the value obtained in a single realization of the system.

On the other hand, variables that are not self-averaging may exhibit fluctuations from one realization to another, and when averaging over the disorder, configurations with zero probability may contribute finite values to the system.

The argument for averaging extensive quantities, initially proposed by Brout [9], considers a system that is very large and can be divided into numerous macroscopic subsystems, each characterized by a different set of disorder variables. Assuming negligible coupling between the subsystems, the value of any normalized extensive variable for the entire system is equal to the average of its values over the subsystems. In practice, if the original system is sufficiently large, the number of subsystems will be large enough that their individual averages will differ only slightly from the average over all realizations of disorder in the complete system.

In the literature, various approaches have been explored to investigate self-averaging properties. For a more detailed discussion and applications, you can refer to references such as [55, 56, 57, 58, 59, 60, 61].

From now on, let us move to a discussion about an example of averaging over the disorder. As mentioned before, the free energy is an extensive quantity, so let us use it as an example. We can start by defining the free energy density for a given disorder realization as follows

$$F(h) = -\frac{1}{\beta V}\ln Z(h), \tag{3.5}$$

where $Z(h)$ is the partition function given by (3.4), and $h$ is one disorder realization. The average over the probability distribution of the disorder is given by

$$\begin{aligned} F =& \mathbb{E}[F(h)] \\ =& \int \mathrm{d}h \; P(h)F(h) \\ =& -\frac{1}{\beta V}\mathbb{E}[\ln Z(h)], \end{aligned} \tag{3.6}$$

where $\mathbb{E}[\cdots]$ denotes the average over all the disorder realizations. In this expression, it is necessary to compute the average of a logarithm, which is not a straightforward task and is quite uncommon in statistical mechanics. This arises from the nature of quenched disorder, which requires us to average extensive quantities like the free energy instead of the partition function, as in the case of annealed disorder. Therefore, the above expression is commonly referred to as the *quenched average*. It is important to note that we have two distinct averages here. The first one is the thermodynamic average over the Boltzmann measure, used to obtain $F(h)$, followed by the average over the disorder. The order of these averages is crucial to obtain the correct result.

Let us briefly discuss the probability distribution in this context. Since we cannot determine the values of the random variables for different realizations, we need to describe them using a probability distribution. Assuming that the degrees of freedom characterizing the disorder exhibit non-long range correlations, we can approximate the probability distribution as a Gaussian one. Thus, the probability can be written as follows

$$P(h) = p\exp\left[-\frac{1}{2\varrho^2}\int \mathrm{d}^{d+1}x\ (h(x))^2\right], \tag{3.7}$$

with $p$ being a normalization factor and $\varrho^2$ a parameter that reflects the strength of the disorder. In this case, we have a delta-correlated random field where the two-point correlation function is given by

$$\mathbb{E}[h(x)h(y)] = \varrho^2\delta^{d+1}(x-y), \tag{3.8}$$

and, as a characteristic of Gaussian distributions, we have that $\mathbb{E}[h(x)] = 0$. Another option for this distribution is given by

$$P(h) = p\exp\left[-\frac{1}{2}\int\int \mathrm{d}^{d+1}x\mathrm{d}^{d+1}y\ h(x)V^{-1}(x-y)h(y)\right], \tag{3.9}$$

with the corresponding correlation function

$$\mathbb{E}[h(x)h(y)] = V(x-y). \tag{3.10}$$

## 3.3 Spin glass model

Before continuing the discussion about methods to evaluate the quenched average, let us take some time to discuss systems with quenched disorder. Glassy systems are a good candidate to use as an example, and we will focus on a specific one, the Spin-Glass model. Spin-glasses have attracted attention in both experimental and theoretical fields as prototypical systems with quenched disorder [1, 2, 62, 63].

Spin-glass systems are magnetic alloys in which magnetic impurities are embedded in a magnetically inert host material. The impurities occupy random positions and are not displaced within the sample on experimental timescales. The interactions between the magnetic moments, or spins, are in conflict with each other due to the presence of frozen-in structural disorder. As a result, a regular long-range ordered state such as ferromagnetic or antiferromagnetic order cannot be established. The theoretical description of spin-glass systems began with the pioneering work of Edwards and Anderson [10].

### 3.3.1 *Edwards-Anderson model*

The mathematical model introduced by Edwards and Anderson to describe spin-glass behavior is a generalization of the well-known Ising model [64]. The Hamiltonian of the spin-glass model can be defined as follows

$$\mathbf{H}(S_i; J_{ij}) = -\sum_{ij} J_{ij} S_i S_j - \sum_i h_i S_i. \tag{3.11}$$

This Hamiltonian describes a system composed of $N$ spins $S_i$ located at the sites $i$ of a regular lattice, where $h_i$ represents a magnetic field interacting locally with the spins. The values of $J_{ij}$ defines the kind of interaction, ferromagnetic or anti-ferromagnetic, being $J_{ij} > 0$ and $J_{ij} < 0$ respectively. The sum in the expression is taken over all pairs $i, j$ of nearest neighbors. The interaction constants $J_{ij}$ between spins located at positions $i$ and $j$ are independent random variables defined by a Gaussian distribution

$$P(J_{ij}) = \sqrt{\frac{N}{2\pi}} e^{-\frac{N}{2\pi}(J_{ij})^2}. \tag{3.12}$$

This model reproduces the two inherent properties that characterize spin-glass systems, the *quenched disorder*, already discussed, and *frustration*. Once the concept of quenched disorder is understood, it is necessary to introduce the notion of frustration. For this, let us consider an arrangement of three spins with interactions $J_{12}$, $J_{23}$, and $J_{13}$ between them. For practical purposes, let us assume that these interactions differ only in their signs and have equal intensity. With this perspective, it is possible to find two essentially different situations corresponding to the ground state. The ground state of this system is unique when the product of all three interactions is positive and will be degenerate if the product is negative. When we go from spin to spin, in the degenerate case, the orientation of one of the spins is not satisfied with respect to the interaction with its neighbors. This implies that if we take a closed spin chain $\mathcal{C}$ with an arbitrary number of couplings, not all interactions can be satisfied if the product of the spin-spin interactions along the chain is negative, then

$$\prod_{\mathcal{C}} J_{12}J_{23}\cdots J_{n1} < 0 \rightarrow \textit{frustration}. \tag{3.13}$$

In fact, any real lattice of two or more dimensions will have a complicated network of interpenetrating frustrated loops, making this matter a topic of current discussion.

### 3.3.2 *Sherrington-Kirkpatrick model*

The Sherrington-Kirkpatrick model is the infinite-range version of the Edwards-Anderson model. This version describes spin-glass systems at low temperature [65]. It was proposed as a mean-field model with all spins interacting with each other. The Hamiltonian for this model is basically the Hamiltonian for the Edwards-Anderson model, eq. (3.11), with a difference in the sum. The sum $\sum_{ij}$ runs over all distinct pairs of spins, $N(N-1)/2$ of them. Due to the fact that each spin interacts with every other spin, the spatial structure of this model is irrelevant for its properties. Here, the space is simply the set of $N$ sites in which the Ising spins are placed, and all these spins could be considered as nearest neighbors. In the thermodynamic limit, where $N \rightarrow \infty$, this structure can be interpreted as an infinite-dimensional lattice. This implies that by making this assumption, the mean-field approach would be exact.

## 3.4 Random field model

### 3.4.1 Random Field Ising Model

In this section, let us discuss one of the most important and relevant models for systems with quenched disorder, the *Random Field Ising Model* (RFIM).

The RFIM was initially introduced by Larkin in the early 1970s [66] and later studied by Imry and Ma [67]. This model includes the presence of a random external magnetic field that opposes the ordering induced by the ferromagnetic spin-spin interaction. The Hamiltonian of the RFIM is defined as follows

$$H = -\sum_{(i,j)} J_{ij} S_i S_j - \sum_i h_i S_j. \tag{3.14}$$

This Hamiltonian describes a system of $N$ spins $S_i$ located at points of a lattice, with $J_{ij}$ representing the positive non-random interaction between spins. In this model, the sum is restricted to the nearest neighbor pairs $(i, j)$, and the fields $h_i$ are independent quenched random variables defined by a Gaussian distribution. The Hamiltonian can be written as

$$P(h_i) = \frac{1}{\sqrt{2\pi\varrho^2}} \exp\left[-\frac{h_i^2}{2\varrho^2}\right], \tag{3.15}$$

with the following two-point correlation function

$$\mathbb{E}(h_i) = 0 \text{ and } \mathbb{E}(h_i h_j) = \varrho^2 \delta_{ij}. \tag{3.16}$$

In both expressions, the $\varrho^2$ represents the variance of the distribution and characterizes the strength of the disorder. In this type of system, long-range and random ordering are in competition, as neighboring spins tend to align parallel while the applied external field tries to fix each spin according to the sign of the local field.

The Hamiltonian (3.14), in general, describes, in a certain way, any solid-state system that has a transition with two degenerate ordered states and contains frozen impurities that locally break the symmetry between these states [68]. For a pure magnetic system, the ordering of spins results from a competition between energy interaction and entropy. In fact, in one dimension, entropy dominates except at absolute zero temperature, and at infinite temperature, the spins are disordered. However, this may not hold if the spin couplings are long-ranged. On the other hand, in all dimensions greater than one, there exists an ordered ferromagnetic phase for the case of the pure Ising model without an external magnetic field. A second-order phase transition takes place at a given critical temperature, below which energy dominates over entropy, and a long-range magnetic order can be established. In most cases, thermal fluctuations easily break up the spin ordering in lower dimensions. This leads to the notion of the lower critical dimension, which is defined as the dimension above which an ordered phase is stable at finite temperature [69].

The presence of a random external magnetic field affects the ordering associated with the ferromagnetic exchange interactions. At low temperatures, the main competition occurs between this type of energy, which contributes to the appearance of long-range order, and the random field, which tries to eliminate such order. Thermal fluctuations become less relevant, so the critical behavior at a possible phase transition would be governed by the fixed point at zero temperature. The random field energy becomes dominant when the strength of the disorder is large compared to the coupling between the spins, resulting in complete disorder of the system. This occurs because the spins will be oriented according to their local field $h_i$ and thus become uncorrelated. In contrast, for a very weak random field, the ferromagnetic ground state becomes unstable, as the transition temperature exhibits a decreasing behavior as the disorder strength increases [1, 3, 8].

In low enough dimensions, the presence of a weak disorder can significantly impact the formation of a long-range ferromagnetic ordered phase. Imry and Ma provided a strong argument on how a robust random field can destroy the ferromagnetic ordering [67]. Further discussions on phase transitions related to the dimensionality of the system can be found in references [70, 71, 72, 73].

### 3.4.2 Random field in the scalar Landau-Ginzburg model

A continuous description of the RFIM is provided by the Landau-Ginzburg model. In this model, the spin variables are replaced by a field coupled to an external quenched disorder field in a d-dimensional Euclidean space. The corresponding Hamiltonian for the $\lambda\phi^4$ theory is defined as [3, 8]:

$$H(\phi, h) = \int \mathrm{d}^{d+1}x \left[ \frac{1}{2}\phi(x)\left(-\Delta + m_0^2\right)\phi(x) + \frac{\lambda}{4!}\left(\phi(x)\phi(x)\right)^2 - h(x)\phi(x) \right], \tag{3.17}$$

where $\phi(x)$ is the field, $h(x)$ is the quenched random field. This can be generalized for multiples fields. The symbol $\Delta$ denotes the Laplacian operator in $\mathbb{R}^d$. The partition function for this case can be written as

$$Z(h) = \int [\mathrm{d}\phi] \exp\left[-H(\phi, h)\right], \tag{3.18}$$

we recall that $\mathrm{d}\phi$ represents the functional measure, as mentioned in the previous chapter. The random variables that characterize the disorder are defined by a Gaussian distribution, just like in the usual random field Ising model. Therefore, we can express the probability of the disorder as follows

$$P(h) \approx \exp\left[-\frac{1}{2\varrho^2}\int \mathrm{d}^{d+1}x\,(h(x))^2\right], \tag{3.19}$$

and we have a delta-correlated random field, where the two-point correlation function is given by

$$\mathbb{E}[h(x)h(y)] = \varrho^2\delta^{d+1}(x-y). \tag{3.20}$$

Now, it is necessary to compute the h-dependent free energy (3.5). The ground state configuration for the system corresponds to the values of the field that minimize the free energy. This is typically determined by solving the saddle-point equation in the presence of a quenched random field,

$$(-\varDelta + m_0^2)\phi(x) + \frac{\lambda}{3!}\phi^3(x) = h(x), \tag{3.21}$$

where the solutions depend on particular configurations of the quenched fields.

Perturbation theory is an inappropriate procedure to be used in systems where the disorder gives rise to a large number of local minima. To overcome this problem, we can perform an average over the disorder for the free energy. Consequently, we have

$$F = \int [\mathrm{d}h]\, P(h)F(h). \tag{3.22}$$

In this case, we are averaging over all realizations of the random function $h(x)$. To perform this average, we will consider two approaches: the *Replica Trick* and the *Distributional Zeta-Function Method*. In the next two sections, both of them will be discussed, and the result for the average will be derived.

## 3.5 The *Replica Trick*

### 3.5.1 A brief discussion about the method

The *Replica trick* was proposed by Edwards and Anderson to study the transition point observed experimentally in the susceptibility of dilute magnetic alloys [10]. The method relies on utilizing a mathematical technique involving replicas of the system and exploits a fundamental property of the logarithm function

$$\ln z = \lim_{n\to 0} \frac{z^n - 1}{n}. \tag{3.23}$$

This property allows us to rewrite (3.6) as

$$F = -\frac{1}{\beta V} \lim_{n\to 0} \frac{\mathbb{E}[Z^n]}{n}. \tag{3.24}$$

This implies that the averaging of the logarithm is reduced to the computation of the average of the partition function. For an integer $n$, this approach necessitates constructing the product of partition functions of $n$ identical and non-interacting copies of the original system, and evaluating the average of the disorder before taking the limit $n \to 0$. From this procedure, the partition function can be written as

$$Z^n = \mathrm{Tr}_{(s^{(a)})} \exp\left[-\beta \sum_{a=1}^{n} H\left(h, s^{(a)}\right)\right], \tag{3.25}$$

where the subscript $(a)$ is the replica index and goes from 1 to $n$. Here, the trace will be the product of sums over each $s^{(a)}$.

As we can see in the above expression, a conceptual difficulty can be noted in the method. The index $(a)$ is an integer that must be sent to zero in the replica limit to maintain agreement with the logarithm property (3.23), where $n$ is a real number. This is a problematic situation resolved by explicitly writing the dependence on $n$ of the replica partition function in such a way that it can be regarded as a continuous parameter [10]. This procedure is not mathematically rigorous and has therefore been the source of much debate and criticism over the years [74, 75, 76, 77]. Despite this, the results obtained with the method are physically meaningful and it has been assumed that it appropriately incorporates physical elements of different systems where it is used. More discussions about the method can be found in references [61, 78, 79]. On the other hand, due to the lack of mathematical rigor in the replica trick, alternative methods have been proposed over the years [11, 12], including the method used in this study, the distributional zeta-function [13].

### 3.5.2 The average free energy in the replica approach

Now, let us return to the computation of the quenched average for the free energy (3.22) using the replica approach. To implement the method, we consider the product of partition functions of $n$ identical and independent replicas, given by

$$Z^n = \int \prod_{i=1}^{n} [\mathrm{d}\phi_i] \exp\left[-\sum_{j=1}^{n}\int \mathrm{d}^{d+1}x \left(\frac{1}{2}\phi_j(x)\left(-\Delta + m_0^2\right)\phi_j(x) + \frac{\lambda}{4!}\phi_j^4(x) - h_j(x)\phi_j(x)\right)\right]. \tag{3.26}$$

By integrating over the disorder distribution, we obtain the replica partition function $Z_n$, which is

$$\begin{aligned} Z_n =& \mathbb{E}[Z^n] \\ =& \int [\mathrm{d}h] \prod_{i=1}^{n} [\mathrm{d}\phi_i] \exp\left[\sum_{j=1}^{n}\int \mathrm{d}^{d+1}x \left(-\frac{1}{2\sigma}h^2(x) + h_j(x)\phi_j(x)\right)\right] \\ & \times \exp\left[-\sum_{j=1}^{n}\int \mathrm{d}^{d+1}x \left(\frac{1}{2}\phi_j(x)\left(-\Delta + m_0^2\right)\phi_j(x) + \frac{\lambda}{4!}\phi_j^4(x)\right)\right]. \end{aligned} \tag{3.27}$$

The $h$-integral can indeed be evaluated as a Gaussian integration. After performing the integration, the resulting form of the partition function becomes

$$Z_n = \int \prod_{i=1}^{n} [\mathrm{d}\phi_i] \exp\left[-H_{eff}(\phi_i)\right], \tag{3.28}$$

with the effective Hamiltonian $H_{eff}$ as

$$H_{eff}(\phi_i) = \frac{1}{2}\sum_{i=1}^{n}\sum_{j=1}^{n}\int \mathrm{d}^{d+1}x \left(\frac{1}{2}\phi_j(x)\left[\left(-\Delta + m_0^2\right)\delta_{ij} - \sigma\right]\phi_j(y)\right) + \frac{\lambda}{4!}\sum_{j=1}^{n}\int \mathrm{d}^d x\phi_j^4(x) \tag{3.29}$$

The saddle point equation for the $n$ replicas is

$$\left(-\Delta + m_0^2\right)\phi_i(x) + \frac{\lambda}{3!}\phi_i^3(x) = \sigma\sum_{j=1}^{n}\phi_j(x). \tag{3.30}$$

If we assume all replicas to be the same, i.e., $\phi_i(x) = \phi(x)$, as would be natural to assume, the equations (3.30) are reduced to

$$\left(-\Delta + \left(m_0^2 - n\sigma\right)\right)\phi(x) + \frac{\lambda}{3!}\phi^3(x) = 0, \tag{3.31}$$

then, by taking the limit $n \to 0$, this equation defines the ground state of a system without disorder, which has the trivial solution $\phi(x) = 0$ for $m_0^2 > 0$. A non-trivial solution can only be obtained if the replicas are not equal, in other words, replica symmetry must be broken [79, 80].

For convenience, instead of working in coordinate space, let us consider a treatment in momentum space. Performing a Fourier transform on the effective Hamiltonian (3.29), we obtain

$$H_{eff}(\phi_i) = \frac{1}{2}\sum_{i,j=1}^{n}\int \frac{\mathrm{d}^{d+1}p}{(2\pi)^d}\phi_i(p)\left[G_0\right]_{ij}^{-1}\phi_j(-p) + \frac{\lambda}{4!}\sum_{j=1}^{n}\phi_j^4, \tag{3.32}$$

where the factor $[G_0]_{ij}^{-1}$ represents the inverse of the two-point correlation function in the three-level approximation, which is defined as

$$\left[G_0\right]_{ij}^{-1}(p) = (p^2 + m_0^2)\delta_{ij} - \sigma. \tag{3.33}$$

To obtain the respective two-point correlation functions, we need to invert the above expression using the projector operators $(P_T)ij$ and $(P_L)ij$, which are

$$(P_T)_{ij} = \delta_{ij} - \frac{1}{n} \text{ and } (P_L)_{ij} = \frac{1}{n}. \tag{3.34}$$

The equation (3.33) can be expressed in terms of both operators as

$$\left[G_0\right]_{ij}^{-1}(p) = (p^2 + m_0^2)\left(\delta_{ij} - \frac{1}{n}\right) + (p^2 + m_0^2 - n\sigma)\frac{1}{n}. \tag{3.35}$$

Now, we can invert the above expression, and the desired result can be achieved as

$$\left[G_0\right]_{ij}(p) = \frac{\delta_{ij}}{p^2 + m_0^2} + \frac{\sigma}{(p^2 + m_0^2)(p^2 + m_0^2 - n\sigma)}. \tag{3.36}$$

The first term corresponds to the bare contribution to the connected two-point correlation function in the absence of the random field. Meanwhile, the second term represents the contribution to the disconnected two-point correlation function, which becomes connected after averaging over the random variable [3].

## 3.6 The *Distributional Zeta-function method*

The authors Svaiter and Svaiter proposed an alternative procedure, called the *Distributional Zeta-Function* method, to compute the average free energy for quenched disorder [13]. To obtain the expression for the average free energy, we consider the Euclidean action functional of a scalar field with the $\lambda\phi^4$ interaction, and the disorder degrees of freedom linearly coupled to the field. This action functional is given by

$$S(\phi, h) = \int \mathrm{d}^{d+1}x\left[\frac{1}{2}\phi(x)\left(-\mathit{\Delta} + m_0^2\right)\phi(x) + \frac{\lambda}{4!}\phi^4(x) - h(x)\phi(x)\right] \tag{3.37}$$

The generalised zeta-function is defined as

$$\zeta_{\mu,f}(s) = \int_{\mathit{\Omega}} f(x)^{-s}\mathrm{d}\mu(x), \tag{3.38}$$

for $s \in \mathbb{C}$ such that $f^{-s} \in L^1(\mu)$. In the formalism for the case $f = Z(h)$ and $d\mu = [dh]\, P(h)$, the distributional zeta-function is defined as

$$\Phi(s) = \int [dh]\, P(h) Z(h)^{-s}. \tag{3.39}$$

Since the part of the action that does not involve disorder is even, then

$$Z(h) = Z(-h) = \frac{Z(h) + Z(-h)}{2}, \tag{3.40}$$

that is equivalent to

$$Z(h) = \int [d\phi] \cosh\left[\int d^{d+1}x\ h(x)\phi(x)\right] \exp\left[-S(\phi)\right], \tag{3.41}$$

where $S(\phi)$ is the action functional for the pure system. As a consequence of the above expression, we have that $Z(h)^{-s} \leqslant Z(0)^{-\mathrm{Re}[s]}$ in the integrand of (3.39) for $\mathrm{Re}[s] \geqslant 0$. This ensures that the integral in (3.39) converges and is well-defined in the half-complex plane. As a result, $\Phi$ is also well-defined in the same region without resorting to analytic continuation [81].

Now taking into account that[1]

$$-\frac{d}{ds}\, Z(h)^{-s}\Big|_{s=0^+} = \ln Z(h), \tag{3.42}$$

we can rewrite (3.2), in this approach, as

$$F = -\frac{d}{ds}\, \Phi(s)\Big|_{s=0^+}. \tag{3.43}$$

Now in order to proceed, lets us perform a Mellin transform to obtain

$$Z(h)^{-s} = \frac{1}{\Gamma(s)} \int_0^\infty dt\ t^{s-1} \exp\left[-Z(h)t\right], \tag{3.44}$$

for $Re[s] > 0$ and $Z(h) > 0$. By replacing (3.44) into (3.39), we obtain

$$\Phi(s) = \frac{1}{\Gamma(s)} \int [dh]\, P(h) \int_0^\infty dt\ t^{s-1} \exp\left[-Z(h)t\right]. \tag{3.45}$$

It follows that, the average for the free energy, (3.43), will be written as

$$F = -\frac{d}{ds}\left[\frac{1}{\Gamma(s)} \int [dh]\, P(h) \int_0^\infty dt\ t^{s-1} \exp\left[-Z(h)t\right]\right]_{s=0^+}. \tag{3.46}$$

[1] $\frac{df}{ds}\Big|_{s=0^+}$ stands for $\lim_{s\to 0^+} \frac{f(s)-f(0)}{s}$.

Now, to continue the evaluation, let us write $\Phi = \Phi_1 + \Phi_2$, where we split the $t$-integrand of $\Phi$ into two intervals $[0, a]$ and $[a, \infty]$, with $a$ being an arbitrary and positive real number. This implies that we can write these as

$$\Phi_1(s) = \frac{1}{\Gamma(s)} \int [\mathrm{d}h]\, P(h) \int_0^a \mathrm{d}t\; t^{s-1} \exp\left[-Z(h)t\right]. \tag{3.47}$$

and

$$\Phi_2(s) = \frac{1}{\Gamma(s)} \int [\mathrm{d}h]\, P(h) \int_a^\infty \mathrm{d}t\; t^{s-1} \exp\left[-Z(h)t\right]. \tag{3.48}$$

As consequence, we can rewrite (3.43) as a sum,

$$F = -\frac{\mathrm{d}}{\mathrm{d}s}\, \Phi_1(s)|_{s=0^+} - \frac{\mathrm{d}}{\mathrm{d}s}\, \Phi_2(s)|_{s=0^+}. \tag{3.49}$$

Now, we can use a series representation for the exponential in (3.47). Since the series converges uniformly for all $h$, we can exchange the order of integration of the sum for the series and the $t$-integral to obtain

$$\Phi_1(s) = \int [\mathrm{d}h]\, P(h) \left[ \frac{1}{\Gamma(s)} \sum_{k=0}^{\infty} \frac{(-1)^k a^{k+s}}{k!(k+s)} Z(h)^k \right]. \tag{3.50}$$

The first term of the series has a singularity at $s = 0$, but it can be removed by invoking the property $\Gamma(s)s = \Gamma(s+1)$. In this way, we can rewrite the above expression as

$$\Phi_1(s) = \frac{a^s}{\Gamma(s+1)} + \frac{1}{\Gamma(s)} \sum_{k=1}^{\infty} \frac{(-1)^k a^{k+s}}{k!(k+s)} \mathbb{E}[Z^k], \tag{3.51}$$

this is valid for $Re[s] > 0$. Now, we perform the differentiation of $\Phi_1$ and obtain

$$-\frac{\mathrm{d}}{\mathrm{d}s}\, \Phi_1(s)|_{s=0^+} = \sum_{k=1}^{\infty} \frac{(-1)^k a^k}{k!k} \mathbb{E}[Z^k] + f(a), \tag{3.52}$$

where

$$f(a) = -(\ln a + \gamma), \tag{3.53}$$

with $\gamma$ being the Euler-Mascheroni constant [82]. And now, taking the derivative of $\Phi_2$, we have

$$-\frac{\mathrm{d}}{\mathrm{d}s}\, \Phi_2(s)|_{s=0^+} = -\int [\mathrm{d}h]\, P(h) \int_a^\infty \mathrm{d}t\; t^{-1} e^{-Z(h)t} = R(a). \tag{3.54}$$

As we can see, the contribution for the average free energy from $\Phi_1$ is written as a series in which all the integer moments of the partition function appear. On the other hand, we do not have an explicit form for the contribution from $\Phi_2$. From the junction of all these equations, we are now able to write the average free energy as

$$F = \sum_{k=1}^{\infty} \frac{(-1)^{k+1} a^k}{k!k} \mathbb{E}[Z^k] - (\ln\, a + \gamma) + R(a) \tag{3.55}$$

where $R(a)$ satisfies the following condition

$$|R(a)| \leqslant \frac{1}{Z(0)a} e^{-Z(0)a}. \tag{3.56}$$

It is important to draw attention to the fact that we cannot take the limit $a \to \infty$ as the above series would become meaningless. However, the contribution of $R(a)$ can be made arbitrarily small by setting $a$ large enough. For a further comparison between this method and the replica trick see ref. [81].

# Chapter 4

# The $\lambda\phi^4$ Euclidean quantum field theory with quenched disorder

In this chapter, the main focus will be the evaluation of the loops described in Chapter 2 in the presence of a quenched disorder. The first part of this chapter will provide a description of the $\lambda\phi^4$ model with the disorder. Subsequent sections will present results and discussions on the effect of this quenched disorder on the renormalized squared mass.

## 4.1 The effective action functional for the quenched disorder system

Systems with quenched disorder were already discussed in the previous chapter. However, in this chapter, we will provide a more detailed discussion about the model. Our first task is to demonstrate the effective action functional for the quenched $\lambda\phi^4$ model using the distributional zeta-functions approach.

Let us start by defining the action functional with the disorder as

$$S(\phi, h) = S(\phi) + \int_0^\beta \mathrm{d}\tau \int \mathrm{d}^d x \; h(\mathbf{x})\phi(\tau, \mathbf{x}), \tag{4.1}$$

where $S(\phi)$ is the action functional for a Euclidean quantum scalar field for the pure system, given by (2.18), and $h(\mathbf{x})$ represents the disorder. In a general situation, a disordered media can be modeled by a real random field $h(\mathbf{x}) = h_\omega(\mathbf{x})$ in $\mathbb{R}^d$, where $\mathbb{E}[h(\mathbf{x})] = 0$ and covariance $\mathbb{E}[h(\mathbf{x})h(\mathbf{y})]$ , where this average is taken over the parameter

$\omega$. Now, let us introduce the disorder generating functional of correlation functions, for one realization of the disorder, with an external source as

$$Z[J,h] = \int [\mathrm{d}\phi] \exp\left[-S(\phi,h) + \int_0^\beta \mathrm{d}\tau \int \mathrm{d}^d x \; J(\tau,\mathbf{x})\phi(\tau,\mathbf{x})\right]. \tag{4.2}$$

As in the pure system, the generating functional of connected correlations functions can be defined as $W[J,h] = lnZ[J,h]$. Now, the average of $W[J,h]$ can be written as

$$\mathbb{E}[W[J,h]] = \int [\mathrm{d}h]\, P(h) W[J,h], \tag{4.3}$$

where $[\mathrm{d}h]$ is a functional measure. In the distributional zeta-functions method, this average will be represented as

$$\mathbb{E}[W[J,h]] = \sum_{q=1}^{\infty} \frac{(-1)^{q+1) a^q}}{q!q} \mathbb{E}[(Z[J,h])^q] - \ln a - \gamma + R(a,J), \tag{4.4}$$

where $R(a,J)$ is given by

$$R(a,J) = -\int [\mathrm{d}h]\, P(h) \int_a^\infty \mathrm{d}t \; t^{-1} \exp\left[-Z[J,h]t\right]. \tag{4.5}$$

To proceed, we absorb $a$ in the functional measure and we assume that the probability distribution of the disorder is written as $[\mathrm{d}h]\, P(h)$, where

$$P(h) = p_0 \exp\left[-\frac{1}{2\varrho^2} \int \mathrm{d}^d x \, (h(\mathbf{x}))^2\right]. \tag{4.6}$$

The quantity $\varrho$ is a positive parameter that is associated with the strength of the disorder and $p_0$ is the normalization factor. In this case we have a delta correlated disorder, (3.20). After integrating over the disorder, we obtain each moment of the partition function as

$$\mathbb{E}[(Z(J,h)^q] = \int \prod_{i=1}^{k} \left[\mathrm{d}\phi_i^{(k)}\right] \exp\left[-S_{eff}\left(\phi_i^{(q)}, J_i^{(q)}\right)\right]. \tag{4.7}$$

The imaginary-time effective action for each moment of the partition function in the presence of a source $J$ can be derived. The new field variables that arise are assumed to satisfy the periodic condition given in section 2.3, i.e., $\phi(\tau,\mathbf{x}) = \phi(\tau+\beta,\mathbf{x})$. Knowing that the disorder field is strongly correlated in the compactified dimension. This implies a nonuniform disorder field $h(\tau,\mathbf{x})$ in the $(d+1)$-dimensional classical Euclidean field theory. In this case, we have an anisotropic delta-correlated disorder field, i.e.,

$$\mathbb{E}[h(\tau,\mathbf{x})h(\tau',\mathbf{x})] = \varrho^2 \delta^d(\mathbf{x}-\mathbf{y}). \tag{4.8}$$

In this case, we obtain a $(d+1)$-dimensional Euclidean space with fields obeying periodic boundary conditions in one spatial coordinate. An effective action will be derived for each moment of the partition function as

$$\begin{aligned} S_{eff}(\phi_i^{(q)}, J_i^{(q)}) =& \frac{1}{2}\int_0^\beta \mathrm{d}\tau \int \mathrm{d}^d x \left[\sum_{i=1}^{q}\left(\phi_i^{(q)}(\tau,\mathbf{x})\left(-\frac{\partial^2}{\partial\tau^2} - \mathbf{\Delta} + m_0^2\right)\phi_i^{(q)}\right.\right. \\ & \left.\left. +\rho_0\left(\phi_i^q(\tau,\mathbf{x})\right)^3 + \frac{\lambda_0}{2}\left(\phi_i^q(\tau,\mathbf{x})\right)^4\right)\right] \\ & - \frac{1}{2}\int_0^\beta \mathrm{d}\tau \int \mathrm{d}^d x \sum_{r,s=1}^{q} \phi_r^{(q)}(\tau,\mathbf{x}) J_s^q(z,\mathbf{x}) \\ & - \frac{\varrho^2}{2\beta^2}\int_0^\beta \mathrm{d}\tau \int_0^\beta \mathrm{d}\tau' \int \mathrm{d}^d x \sum_{r,s=1}^{q} \phi_r^{(q)}(\tau,\mathbf{x})\phi_s^{(q)}(\tau',\mathbf{x}) \end{aligned} \tag{4.9}$$

where the field variables and sources are assumed to satisfy the previously mentioned periodic boundary conditions. As we can see, the last term of (4.9) represents a non-local contribution [38].

In order to define the propagator for this system, careful attention is required to understand the consequences of randomness in a quantum system at low temperatures in the spontaneously broken phase. However, for practical purposes, this discussion will be omitted in this work, and only the form of the propagator will be presented. The propagator for this system in the low-temperature case is defined as

$$\Delta_\beta(\mathbf{p},\omega_n,\sigma_n) = \frac{1}{(\mathbf{p}^2 + m_0^2 + \omega_n^2 + \sigma_n)} \tag{4.10}$$

where

$$\sigma_n = \frac{2\pi|n|}{\beta}q\varrho^2 \tag{4.11}$$

and $\omega_n$ is the Matsubara frequency term for the scalar field, given by

$$\omega_n = \frac{2\pi n}{\beta}. \tag{4.12}$$

The method to obtain this propagator is extensively discussed by Heymans [38].

## 4.2 One-loop Evaluation

The renormalized squared mass $m_R^2(\beta, q, \mu)$ in the $k$th moment is similar to the case discussed in section 2.5. The renormalized mass squared is given by

$$m_R^2(\beta,q,\mu) = m_0^2 + \delta m_0^2 + f_1 \Delta m_1^2(\beta,q,\mu) + f_2\Delta m_2^2(\beta,q,\mu), \tag{4.13}$$

Where $f_i$ are the symmetric factors, and the mass counterterm has been introduced. In the context described in sec. 2.5, $\varDelta m_1^2$ represents the contribution from the tadpole diagram, as shown in fig. 2.2-a. The second term, $\varDelta m_2^2$, is associated with the contribution from the bubble diagram. The subscript indicating the dimension dependence of the correction terms has been omitted for simplicity. Similar to sec. 2.5, let us begin by defining the mass correction, in the first order of $\lambda$, for the disordered case as

$$\varDelta m_s^2(\beta, q, \mu) = \frac{F(\lambda,\mu,s)}{\beta} \sum_{n\in\mathbb{Z}} \int \frac{\mathrm{d}^d p}{(2\pi)^d} \frac{1}{\left(\mathbf{p}^2 + m_0^2 + \omega_n^2 + \sigma_n\right)^s}, \tag{4.14}$$

where $F(\lambda,\mu,s)$ is a coupling constant that depends on the evaluated loop. Now, we can rewrite the above expression by performing some variable changes and rearrangement, as

$$\varDelta m_s^2(\beta, q, \mu) = \frac{F(\lambda,\mu,s)\beta}{2^{d+1}\pi^{\frac{d}{2}+1}\varGamma\left(\frac{d}{2}\right)} \int_0^\infty \mathrm{d}p\ p^{d-1} \sum_{n\in\mathbb{Z}} \left(\pi n^2 + \frac{\beta^2}{4\pi}\left(p^2+m_0^2\right) + \frac{\beta}{2} q\varrho^2 |n|\right)^{-s}. \tag{4.15}$$

Here, we will apply a Mellin transform and obtain

$$\begin{aligned}\varDelta m_s^2(\beta, q, \mu) = {}& \frac{F(\lambda,\mu,s)\beta}{2^{d+1}\pi^{\frac{d}{2}+1}\varGamma\left(\frac{d}{2}\right)\varGamma(s)} \sum_{n\in\mathbb{Z}} \int_0^\infty \mathrm{d}p\ p^{d-1} \int_0^\infty \mathrm{d}t\ t^{s-1} \\ & \times \exp\left[-\left(\pi n^2 + \frac{\beta^2}{4\pi}\left(p^2+m_0^2\right) + \frac{\beta}{2} q\varrho^2|n|\right)t\right].\end{aligned} \tag{4.16}$$

Before compute the $p$-integral, we can define a dimensionless quantity $r^2 = \frac{\beta^2 p^2}{4\pi}$. Then the above equation can be rewritten as

$$\begin{aligned}\varDelta m_s^2(\beta, q, \mu) = {}& \frac{F(\lambda,\mu,s)\beta^{1-d}}{2\pi\varGamma\left(\frac{d}{2}\right)\varGamma(s)} \sum_{n\in\mathbb{Z}} \int_0^\infty \mathrm{d}r\ r^{d-1} \int_0^\infty \mathrm{d}t\ t^{s-1} \\ & \times \exp\left[-\left(\pi n^2 + r^2 + \frac{\beta^2}{4\pi}m_0^2 + \frac{\beta}{2} q\varrho^2|n|\right)t\right].\end{aligned} \tag{4.17}$$

And finally, we can perform the $r$-integral to obtain

$$\begin{aligned}\varDelta m_s^2(\beta, q, \mu) = {}& \frac{F(\lambda,\mu,s)\beta^{1-d}}{2\pi\varGamma(s)} \int_0^\infty \mathrm{d}t\ t^{s-\frac{d}{2}-1} \exp\left[-\frac{m_0^2\beta^2}{4\pi}t\right] \\ & \times \sum_{n\in\mathbb{Z}} \exp\left[-\left(\pi n^2 + \frac{\beta}{2} q\varrho^2|n|\right)t\right].\end{aligned} \tag{4.18}$$

As we can see, up until this point, we have followed the same process demonstrated in sec. 2.5. However, we observe that the anisotropic disorder introduces a contribution involving $|n|$ into the correlation function. This contribution was not present in the pure system. This implies that we need a different approach to deal with the renormalization of the one-loop. Let us split the summation into two contributions, one for $n = 0$ and another for $n \neq 0$, denoted as $\varDelta m_s^2(\beta, q, \mu)|n = 0$ and $\varDelta m_s^2(\beta, q, \mu)|n \neq 0$, respectively. We will start with $\varDelta m_s^2(\beta, q, \mu)|_{n=0}$ by expressing this contribution as.

$$\varDelta m_s^2(\beta, q, \mu)|_{n=0} = \frac{F(\lambda, \mu, s)\beta^{1-d}}{2\pi\varGamma(s)} A(s, d) \tag{4.19}$$

where

$$A(s, d) = \int_0^\infty \mathrm{d}t\ t^{s-\frac{d}{2}-1} \exp\left[-\frac{\beta^2}{4\pi} m_0^2 t\right] \tag{4.20}$$

For certain values of $d$ and $s$, this integral exhibits an infrared divergence. The integral is defined for $Re[s] > \frac{d}{2}$ and can be analytically continued to $Re[s] > \frac{d}{2} - 1$ for $s \neq \frac{d}{2}$. To handle this situation, we can employ the following approach [83]

$$\int_0^\infty \mathrm{d}x\ x^\lambda \phi(x) = \int_0^1 \mathrm{d}x\ x^\lambda (\phi(x) - \phi(0)) + \int_0^\infty \mathrm{d}x\ x^\lambda \phi(x) + \frac{\phi(0)}{\lambda + 1}, \tag{4.21}$$

is possible to write a renormalized $A(s, d)$ as

$$\begin{aligned} A_R(s, d) = &\int_0^1 \mathrm{d}t\ t^{s-\frac{d}{2}-1} \left(\exp\left[-\frac{\beta^2}{4\pi} m_0^2 t\right] - 1\right) \\ &+ \int_1^\infty \mathrm{d}t\ t^{s-\frac{d}{2}-1} \exp\left[-\frac{\beta^2}{4\pi} m_0^2 t\right] + \frac{2}{2s - d}. \end{aligned} \tag{4.22}$$

Which is valid for $Re[s] > \frac{d}{2}$. For $Re[s] > \frac{d}{2} - 1$ and $s \neq \frac{d}{2}$, the right side of $A_R(s, d)$ exists and defines a regularization of the original integral. Now, let us consider the contribution for $n \neq 0$

$$\begin{aligned} \varDelta m_s^2(\beta, q, \mu) = &\frac{F(\lambda, \mu, s)\beta^{1-d}}{2\pi\varGamma(s)} \int_0^\infty \mathrm{d}t\ t^{s-\frac{d}{2}-1} \exp\left[-\frac{m_0^2\beta^2}{4\pi} t\right] \\ &\times \sum_{n=1}^\infty \exp\left[-\left(\pi n^2 + \frac{\beta}{2} q\varrho^2 |n|\right) t\right]. \end{aligned} \tag{4.23}$$

In the series representation for the free energy with $q = 1, 2, \ldots,$ we find that moments of the partition function corresponding to certain values of $q$ are critical. Specifically, for moments such that $q_{(Q)} = \left[\left(\frac{2\pi Q}{\beta}\right)\frac{2}{\varrho}\right]$ with $Q \in \mathbb{N}$, they exhibit critical behavior. Since our focus is on critical behavior, we will concentrate on this set of critical momenta. Now, we can rewrite (4.23) to accommodate this new definition, and by performing some rearrangements, we obtain

$$\begin{aligned} \varDelta m_s^2(\beta, q, \mu)|_{n\neq 0} = &\frac{F(\lambda, \mu, s)\beta^{1-d}}{2\pi\varGamma(s)} \int_0^\infty \mathrm{d}t\ t^{s-\frac{d}{2}-1} \exp\left[-\pi\left(\frac{m_0^2\beta^2}{4\pi^2} - Q^2\right) t\right] \\ &\times \sum_{n=1}^\infty \exp\left[-\pi (n + Q)^2 t\right] \end{aligned} \tag{4.24}$$

By choosing a specific value of $Q$ as $Q = \frac{\beta}{2\pi} m_0$, we can determine the critical value of $q_c$. The interpretation of this result is that within the infinite number of moments that define the free energy, there exists a subset of critical momenta. Within this subset, there is a particular set characterized by specific values of $Q$ that exhibit the tree-level behavior [38]. With this understanding and interpretation of the specific $Q$ values, we can rewrite (4.24) as

$$\Delta m_s^2(\beta, q_0, \mu)|_{n\neq 0} = \frac{F(\lambda, \mu, s)\beta^{1-d}}{2\pi\Gamma(s)} \int_0^\infty \mathrm{d}t\ t^{s-\frac{d}{2}-1} \sum_{n=1}^{\infty} \exp\left[-\pi (n+Q_0)^2 t\right]. \tag{4.25}$$

Now, we can expand this expression to include the $n = 0$ term. By doing this, the term $\Delta m_s^2(\beta, q, \mu)|_{n\neq 0}$ can be given by.

$$\Delta m_s^2(\beta, q_0, \mu)|_{n\neq 0} = \frac{F(\lambda, \mu, s)\beta^{1-d}}{2\pi\Gamma(s)} \left[\int_0^\infty \mathrm{d}t\ t^{s-\frac{d}{2}-1} \sum_{n=0}^{\infty} e^{-\pi(n+Q_0)^2 t} - A_R(s,d)\right]. \tag{4.26}$$

In order to proceed, let us perform the inverse Mellin transform into the $t$-integral

$$\int_0^\infty \mathrm{d}t\ t^{s-\frac{d}{2}-1} \sum_{n=0}^{\infty} e^{-\pi(n+Q)^2 t} = \Gamma\left(s - \frac{d}{2}\right) \pi^{\frac{d}{2}-s} \sum_{n=0}^{\infty} (n+Q)^{d-2s}. \tag{4.27}$$

And now, our renormalized mass correction will be written as

$$\Delta m_s^2(\beta, q_0, \mu)|_{n\neq 0} = \frac{F(\lambda, \mu, s)\beta^{1-d}}{2\pi\Gamma(s)} \left[\Gamma\left(s - \frac{d}{2}\right) \pi^{\frac{d}{2}-s}\, \zeta\left(2s-d, q_0\right) - A_R(s,d)\right] \tag{4.28}$$

where $\zeta(z, a)$ is the Hurwitz-zeta function

$$\zeta(z,a) = \sum_{n=0}^{\infty} (n+a)^{-z}, \tag{4.29}$$

and an important formula that must be used in the renormalization process is

$$\lim_{z\to 1}\left[\zeta(z,a) - \frac{1}{z-1}\right] = -\psi(a), \tag{4.30}$$

where $\psi(a)$ is the digamma function defined as $\psi(z) = \frac{\mathrm{d}}{\mathrm{d}z}\left[\ln\Gamma(z)\right]$. For a fixed value of $q_0$, the renormalized squared mass will vanish for a family of temperatures. This was proven by Heymans et. al. [38]. In the next section, we will discuss the two-loops using the procedure described in this section.

## 4.3 Two loop evaluation

As already discussed in chapter 2, we have three contributions to the renormalized squared mass when we expand to order $\lambda^2$, as shown in figure 2.2. In this scenario, the renormalized squared mass can be written as

$$m_R^2(\beta,q,\mu) = m_0^2 + \delta m_0^2 + f_{(2)}\Delta m_{(2)}^2(\beta,q,\mu) + f_{(3)}\Delta m_{(3)}^2(\beta,q,\mu), \tag{4.31}$$

where $f_{(i)}$ are the symmetric factor for each loop contribution. In here, all three diagrams will be evaluated in separated subsections for simplification.

### 4.3.1 *Double-Tadpole*

The first of the two-loop diagrams that we will discuss is the double-tadpole diagram. Although this diagram does not contribute to the renormalized squared mass, we will examine it to demonstrate the applicability of the method to this simple two-loop case. Since the double-tadpole diagram is a 1PR diagram, we can separate the two loops by cutting the external leg between them and evaluate each branch separately, as shown in figure 2.2-b. Both loops will have the same form as the tadpole diagram but with different coupling constants. Let us start by writing the expressions for both loops, after applying the Mellin transform and performing the momentum integrals, as follows

$$\Delta m_{(1),(\frac{1}{2})}^2(\beta,q,\mu) = F_{(\frac{1}{2})} \sum_{n_{(\frac{1}{2})}\in\mathbb{Z}} \int_0^\infty \mathrm{d}t\ t^{\frac{d}{2}} \exp\left[-\frac{m_0^2\beta^2 t}{4\pi}\right] \exp\left[-\left(\pi n_{(\frac{1}{2})}^2 - \frac{\beta}{2}q\varrho^2\left|n_{(\frac{1}{2})}\right|\right)t\right], \tag{4.32}$$

where $F = F(\lambda,\beta,\mu)$ is the coupling constant, and the subscript $(\frac{1}{2})$ indicates each loop of the diagram. However, we can drop the distinction between the loops since both of them have the same form and are independent of each other. Now, let us consider $\Delta m_{(1),1}^2$ as

$$\Delta m_{(1)}^2(\beta,q,\mu) = F_1 \sum_{n\in\mathbb{Z}} \int_0^\infty \mathrm{d}t\ t^{\frac{d}{2}} \exp\left[-\frac{m_0^2\beta^2 t}{4\pi}\right] \exp\left[-\left(\pi n^2 - \frac{\beta}{2}q\varrho^2\left|n\right|\right)t\right]. \tag{4.33}$$

It is easy to see that the above expression is the same as (4.18) with $s = 1$. As a consequence, the result after all the procedures will be the same as the one obtained for the one-loop case. This result is expected since this diagram is a trivial one. Both $F$-factors will be the same as in chapter 2, i.e., they are disorder-independent and are defined by

$$F_1(\lambda,\beta,\mu) = -\frac{3\lambda_R^2}{2(4\pi)^3}\frac{(\mu^2)^{4-d}}{4-d}\beta^{1-d}, \tag{4.34}$$

$$F_2(\lambda,\beta,\mu) = -\frac{\lambda_R^2 m_R^2}{2(4\pi)^3}\frac{(\mu^2)^{4-d}}{4-d}\beta^{1-d}. \tag{4.35}$$

All the procedure of the previous section can be applied with $s=1$. Then, the contribution for the renormalized mass from this diagram will be written as

$$\begin{aligned}\varDelta m^2_{(1),1}(\beta,q_0,\mu)|_{n_1\neq 0} = &-\frac{3\lambda_R^2}{(4\pi)^4}\frac{(\mu^2)^{4-d}}{4-d}\beta^{1-d}\\ &\times\left[\varGamma\left(1-\frac{d}{2}\right)\pi^{\frac{d}{2}-1}\,\zeta\left(2-d,q_0\right)-A_R(1,d)\right],\end{aligned} \tag{4.36}$$

$$\begin{aligned}\varDelta m^2_{(1),2}(\beta,q_0,\mu)|_{n_2\neq 0} = &-\frac{\lambda_R^2 m_R^2}{(4\pi)^4}\frac{(\mu^2)^{4-d}}{4-d}\beta^{1-d}\\ &\times\left[\varGamma\left(1-\frac{d}{2}\right)\pi^{\frac{d}{2}-1}\,\zeta\left(2-d,q_0\right)-A_R(1,d)\right],\end{aligned} \tag{4.37}$$

where $A_R(1,d)$ is the renormalized zero frequency term

$$\begin{aligned}A_R(1,d) = &\int_0^1 \mathrm{d}t\; t^{\frac{d}{2}}\left(\exp\left[-\frac{\beta^2}{4\pi}m_0^2 t\right]-1\right)\\ &+\int_1^\infty \mathrm{d}t\; t^{\frac{d}{2}}\exp\left[-\frac{\beta^2}{4\pi}m_0^2 t\right]+\frac{2}{2-d}.\end{aligned} \tag{4.38}$$

### 4.3.2 *Double Scoop*

The next two-loop correction for the renormalized mass will arise from the double-scoop diagram, as shown in Figure 2.2-c. As we know, in this diagram, we cannot disconnect the loops as in the previous case. However, this is also a trivial diagram, which means that the procedure from the previous section can be applied with some rearrangement needed. First of all, let us write the expression for this diagram

$$\begin{aligned}\varDelta m^2_{(2)}(\beta,q,\mu) = &\frac{\lambda_R^2(\mu^2)^{4-d}\beta^2}{4\left(2^{d+1}\pi^{\frac{d}{2}+1}\varGamma\left(\frac{d}{2}\right)\right)^2}\sum_{n,r\in\mathbb{Z}}\int_0^\infty \mathrm{d}k\; k^{d-1}\left(\pi n^2+\frac{\beta^2}{4\pi}\left(k^2+m_0^2\right)+\frac{\beta}{2}q\varrho^2|n|\right)^{-1}\\ &\times\int_0^\infty \mathrm{d}l\; l^{d-1}\left(\pi r^2+\frac{\beta^2}{4\pi}\left(l^2+m_0^2\right)+\frac{\beta}{2}q\varrho^2|r|\right)^{-2}.\end{aligned} \tag{4.39}$$

As we can see, in this diagram we have two momenta and two frequencies, which can be treated independently. For practical purposes, we can define two dimensionless variables:

$K^2 = \frac{\beta^2}{4\pi}k^2$ and $L^2 = \frac{\beta^2}{4\pi}l^2$. After some rearrangement, we obtain

$$\Delta m^2_{(2)}(\beta,q,\mu) = \lambda^2_R(\mu^2)^{4-d}\left(\frac{\beta^{1-d}}{4\pi\Gamma\left(\frac{d}{2}\right)}\right)^2 \sum_{n,r\in\mathbb{Z}}\int_0^\infty \mathrm{d}K\ K^{d-1}\left(\pi n^2 + K^2 + \frac{\beta^2}{4\pi}m_0^2 + \frac{\beta}{2}q\varrho^2|n|\right)^{-1}$$
$$\times\int_0^\infty \mathrm{d}L\ L^{d-1}\left(\pi r^2 + L^2 + \frac{\beta^2}{4\pi}m_0^2 + \frac{\beta}{2}q\varrho^2|r|\right)^{-2}. \tag{4.40}$$

Now we can perform the Mellin transform with $s = 1$ and $s = 2$ for the $k$-integrand and $l$-integrand, respectively,

$$\begin{aligned}\Delta m^2_{(2)}(\beta,q,\mu) =& \lambda^2_R(\mu^2)^{4-d}\left(\frac{\beta^{1-d}}{4\pi\Gamma\left(\frac{d}{2}\right)}\right)^2 \\ &\times\sum_{n\in\mathbb{Z}}\int_0^\infty \mathrm{d}K\ K^{d-1}\int_0^\infty \mathrm{d}t_1 \exp\left[-\left(\pi n^2 + K^2 + \frac{\beta^2}{4\pi}m_0^2 + \frac{\beta}{2}q\varrho^2|n|\right)t_1\right] \\ &\times\sum_{r\in\mathbb{Z}}\int_0^\infty \mathrm{d}L\ L^{d-1}\int_0^\infty \mathrm{d}t_2 t_2 \exp\left[-\left(\pi r^2 + L^2 + \frac{\beta^2}{4\pi}m_0^2 + \frac{\beta}{2}q\varrho^2|r|\right)t_2\right],\end{aligned} \tag{4.41}$$

and now to proceed, we just need to perform the both $K$ and $L$ integral that is an easy task, after this we will get

$$\Delta m^2_{(2)}(\beta,q,\mu) = \lambda^2_R(\mu^2)^{4-d}\left(\frac{\beta^{1-d}}{4\pi}\right)^2\int_0^\infty \mathrm{d}t_1\ t_1^{-\frac{d}{2}}\exp\left[-\frac{\beta^2}{4\pi}m_0^2 t_1\right]\sum_{n\in\mathbb{Z}}\exp\left[-\left(\pi n^2 + \frac{\beta}{2}q\varrho^2|n|\right)t_1\right]$$
$$\times\int_0^\infty \mathrm{d}t_2\ t_2^{1-\frac{d}{2}}\exp\left[-\frac{\beta^2}{4\pi}m_0^2 t_2\right]\sum_{r\in\mathbb{Z}}\exp\left[-\left(\pi r^2 + \frac{\beta}{2}q\varrho^2|r|\right)t_2\right] \tag{4.42}$$

And here we can notice that the first integral in the above expression is simply the (4.18) for $s = 1$, and the second integral is for the analytic continuation of (4.18) for $s = 2$. This is expected because this diagram is also a trivial one. All we need to do now is evaluate the first integral in the same way as in the one-loop case and perform an analytic continuation for the second integral.

Now, let us split $\Delta m^2_{(2)}(\beta,q,\mu)$ into two cases: $n,r = 0$ and $n,r \neq 0$. The contribution $\Delta m^2_{(2)}(\beta,q,\mu)|_{n,r=0}$ can be written as the sum of contributions from both zero frequencies with $s = 1$ and $s = 2$. Specifically, we have

$$\Delta m^2_{(2)}(\beta,q,\mu)|_{n,r=0} = \lambda^2_R(\mu^2)^{4-d}\left(\frac{\beta^{1-d}}{4\pi}\right)^2\ A_R(1,d)\ A'_R(2,d). \tag{4.43}$$

In this case, the $A'_R(s,d)$ represents the analytic continuation of $A(s,d)$, following the same approach as in Section 4.2. However, in this case, we need to extend it to accommodate

$s = 2$. Thus, we have

$$\begin{aligned} A'_R(s,d) = &\int_0^1 \mathrm{d}t\ t^{s-\frac{d}{2}-1}\left(\exp\left[-\frac{\beta^2}{4\pi}m_0^2 t\right] - 1 + \frac{\beta^2}{4\pi}m_0^2\ t\right) \\ &+ \int_1^\infty \mathrm{d}t\ t^{s-\frac{d}{2}-1}\exp\left[-\frac{\beta^2}{4\pi}m_0^2 t\right] + \frac{2}{s-d} + \frac{2}{2s+2-d}. \end{aligned} \tag{4.44}$$

This expression is valid for $Re[s] > \frac{d}{2} - 2$ for $s \neq \frac{d}{2} - 1$ and $s \neq \frac{d}{2}$. Now, we proceed with the $n, r \neq 0$. The $\Delta m^2_{(2)}(\beta, q, \mu)|_{n,r\neq 0}$ will be defined as

$$\begin{aligned} \Delta m^2_{(2)}(\beta,q,\mu)|_{n,r=0} =&\lambda_R^2(\mu^2)^{4-d}\left(\frac{\beta^{1-d}}{4\pi}\right)^2 \\ &\times \int_0^\infty \mathrm{d}t_1\ t_1^{-\frac{d}{2}}\exp\left[-\pi\left(\frac{\beta^2}{4\pi^2}m_0^2 - Q^2\right)t_1\right]\sum_{n=1}^\infty \exp\left[-\pi\left(n+Q\right)^2 t_1\right] \\ &\times \int_0^\infty \mathrm{d}t_2\ t_2^{1-\frac{d}{2}}\exp\left[-\pi\left(\frac{\beta^2}{4\pi^2}m_0^2 - Q^2\right)t_2\right]\sum_{r=1}^\infty \exp\left[-\pi\left(r+Q\right)^2 t_2\right]. \end{aligned} \tag{4.45}$$

By choosing the particular value for $Q = \frac{\beta^2}{4\pi^2}m_0^2$, as already discussed on sec. 4.2, the desired form of $\Delta m^2_{(2)}(\beta, q, \mu)|_{n,r=0}$ will be achieved,

$$\begin{aligned} \Delta m^2_{(2)}(\beta,q_0,\mu)|_{n,r=0} = \lambda_R^2(\mu^2)^{4-d}\left(\frac{\beta^{1-d}}{4\pi}\right)^2 &\int_0^\infty \mathrm{d}t_1\ t_1^{-\frac{d}{2}}\sum_{n=1}^\infty \exp\left[-\pi\left(n+Q_0\right)^2 t_1\right] \\ \times &\int_0^\infty \mathrm{d}t_2\ t_2^{1-\frac{d}{2}}\sum_{r=1}^\infty \exp\left[-\pi\left(r+Q_0\right)^2 t_2\right], \end{aligned} \tag{4.46}$$

the zeroth term of both frequencies can be included, and we obtain

$$\begin{aligned} \Delta m^2_{(2)}(\beta,q_0,\mu)|_{n,r=0} = \lambda_R^2(\mu^2)^{4-d}\left(\frac{\beta^{1-d}}{4\pi}\right)^2 &\left[\int_0^\infty \mathrm{d}t_1\ t_1^{-\frac{d}{2}}\sum_{n\in\mathbb{Z}} \exp\left[-\pi\left(n+Q_0\right)^2 t_1\right] - A_R(1,d)\right] \\ \times &\left[\int_0^\infty \mathrm{d}t_2\ t_2^{1-\frac{d}{2}}\sum_{r\in\mathbb{Z}} \exp\left[-\pi\left(r+Q_0\right)^2 t_2\right] - A'_R(2,d)\right]. \end{aligned} \tag{4.47}$$

As we can see, both integrals have the form of (4.26), as expected. We can verify that for both integrals in (4.47), the result of (4.26) will be achieved. However, in this case, we need to consider the case for $s = 2$, so an analytic continuation is needed. Therefore, we can write $\Delta m_l^2(\beta, q_0, \mu)|_{n\neq 0}$ as

$$\begin{aligned} \Delta m^2_{(2)}(\beta,q_0,\mu)|_{n,r=0} = \lambda_R^2(\mu^2)^{4-d}\left(\frac{\beta^{1-d}}{4\pi}\right)^2 &\left[\Gamma\left(1-\frac{d}{2}\right)\pi^{\frac{d}{2}-1}\,\zeta\left(2-d,q_0\right) - A_R(1,d)\right] \\ \times &\left[\Gamma\left(2-\frac{d}{2}\right)\pi^{\frac{d}{2}-2}\,\zeta\left(4-d,q_0\right) - A'_R(2,d)\right]. \end{aligned} \tag{4.48}$$

The Hurwitz zeta function for $s = 1$ has a simple pole at $z = 1$. Therefore, for $s = 1$ and $d = 3$, the first zeta term in the above equation is finite. However, for $s = 2$, this is not the case. We need to provide an analytic continuation for the Hurwitz zeta function that is valid for $s = 2$. In this case, we can write the zeta function in the following integral representation

$$\zeta(z, a) = -\frac{\Gamma(1-z)}{2\pi i} \int_{\mathcal{C}} \mathrm{d}t \frac{(-t)^{z-1} e^{-at}}{1-e^{-t}}, \tag{4.49}$$

where $\mathcal{C}$ is the Hankel contour.

### 4.3.3 *Sunset*

The last of the two-loop corrections arises from the sunset diagram. Unlike the previous cases, this diagram cannot be treated using the approach presented in section 2.5. The interconnection between the three momenta in this diagram makes it more challenging to evaluate. Let us write down the expression for this diagram in the quenched disorder scenario

$$\begin{aligned} \Delta m^2_{(3)}(\beta, q, \mu) = \frac{\lambda_R^2 (\mu^2)^{4-d}}{6\beta^2} & \sum_{n,r\in\mathbb{Z}} \int \frac{\mathrm{d}^d k}{(2\pi)^d} \int \frac{\mathrm{d}^d l}{(2\pi)^d} \\ & \times \frac{\left( \left[\mathbf{k}^2 + m_0^2 + \omega_n^2 + \sigma_n\right] \left[\mathbf{l}^2 + m_0^2 + \omega_r^2 + \sigma_r\right] \right)^{-1}}{\left( [\mathbf{p} - \mathbf{k} - \mathbf{l}]^2 + m_0^2 + \omega^2_{(t-n-r)} + \sigma_{(t-n-r)} \right)}. \end{aligned} \tag{4.50}$$

To evaluate this diagram, we can take two approaches. One made by Braden [37], presented in chapter 2, for the non disorder case. However, applying this approach to the quenched disorder case leads to a complicated analysis. Therefore, we will use another approach, namely Feynman parametrization [41], as it appears to be more suitable for this scenario.

After applying the Feynman parametrization , the three propagators in the diagram will be combined into a single expression. In other words, we can write the diagram as follows

$$\begin{aligned} \int \frac{\mathrm{d}^d k}{(2\pi)^d} \int \frac{\mathrm{d}^d l}{(2\pi)^d} & \frac{\left( \left[\mathbf{k}^2 + m_0^2 + \omega_n^2 + \sigma_n\right] \left[\mathbf{l}^2 + m_0^2 + \omega_r^2 + \sigma_r\right] \right)^{-1}}{\left( [\mathbf{p} - \mathbf{k} - \mathbf{l}]^2 + m_0^2 + \omega^2_{(t-n-r)} + \sigma_{(t-n-r)} \right)} = \\ & = \Gamma(3-d) \int_0^1 \int_0^1 \mathrm{d}x \mathrm{d}y \frac{[(1-x)x]^{\frac{d-3}{2}}}{y^{\frac{d-1}{2}}} \\ & \times \left( \frac{1}{\mathbf{p}_{eff}^2 + m_{eff}^2 + N^2(1-y) + R^2 \frac{y}{x} + T^2 \frac{y}{1-x}} \right)^{3-d}. \end{aligned} \tag{4.51}$$

where

$$\begin{aligned} m_{eff}^2 =& m_0^2\left(1-y+\frac{y}{x(1-x)}\right); && (4.52)\\ \mathbf{p}_{eff}^2 =& \mathbf{p}^2 y(1-y); && (4.53)\\ N^2 =& \omega_n^2+\sigma_n; && (4.54)\\ R^2 =& \omega_r^2+\sigma_r; && (4.55)\\ T^2 =& \omega_{(t-n-r)}^2+\sigma_{(t-n-r)}. && (4.56) \end{aligned}$$

By performing the Mellin transform and Poisson summation, we obtain the following expression after some rearrangement

$$\begin{aligned} \varDelta m_{(3)}^2(\beta,q,\mu) =& \frac{\lambda_R^2(\mu^2)^{4-d}}{32(4\pi)^d}\left(\frac{1}{\beta^2}\right)^{d-1}\int_0^1 \mathrm{d}x\mathrm{d}y\frac{((1-x)x)^{\frac{d-3}{2}}}{y^{\frac{d-1}{2}}}\int_0^\infty \mathrm{d}z\ z^{1-d}\\ &\times\exp\left[-\frac{\beta^2}{4\pi}\left[m_{eff}^2+\mathbf{p}_{eff}^2\right]z\right]\\ &\times\sum_{n,r\in\mathbb{Z}}\exp\left[-\frac{\pi}{z}\left[n^2+r^2\frac{x(x(y-1)+1)}{y}-2nrx\right]\right]\\ &\times\exp\left[-\beta p_0\left[i\left[rx(1-y)+ny\right]+\frac{3\beta q\varrho^2}{4\pi}zy(1-y)\right]\right]\\ &\times\exp\left[\frac{i}{2}q\beta\varrho^2\left[n(1-3y)+r(1+3x(y-1))\right]\right]\\ &\times\exp\left[\frac{\pi}{4}\left(\frac{q\beta\varrho^2}{2\pi}\right)^2\frac{(x^2\left[-9y^2+10y-1\right]+x\left[9y^2-10y+1\right]+y)}{(x-1)x}z\right] \end{aligned} \tag{4.57}$$

To proceed, let us split this mass correction contribution into two regions: the terms corresponding to zero frequencies $n$ and $r$, and the terms corresponding to nonzero frequencies. We denote these contributions as $\varDelta m_{(3)}^2(\beta,q,\mu)|n,r=0$ and $\varDelta m^2(3)(\beta,q,\mu)|n,r\neq 0$, respectively. However, before continuing, let us use the definition of $Q$ presented in Section 4.2. This allows us to write both cases in a simpler form. Now, considering $n,r=0$, we can write $\varDelta m^2(3)(\beta,q,\mu)|_{n,r=0}$ as

$$\begin{aligned} \varDelta m_{(3)}^2(\beta,q,\mu)|_{n,r=0} =& \frac{\lambda_R^2(\mu^2)^{4-d}}{32(4\pi)^d}\left(\frac{1}{\beta^2}\right)^{d-1}\int_0^1 \mathrm{d}x\mathrm{d}y\frac{((1-x)x)^{\frac{d-3}{2}}}{y^{\frac{d-1}{2}}}\int_0^\infty \mathrm{d}z\ z^{1-d}\\ &\times\exp\left[-\left(\frac{\beta^2}{4\pi}m_{eff}^2-Q_{m_0}^2\right)z\right]\\ &\times\exp\left[-\left(\frac{\beta^2}{4\pi}\mathbf{p}_{eff}^2+Q_{\mathbf{p}}^2\right)z\right], \end{aligned} \tag{4.58}$$

where

$$Q_{m_0}^2 = \frac{\pi}{4} Q^2 \frac{\left(x^2\left[-9y^2+10y-1\right]+x\left[9y^2-10y+1\right]+y\right)}{(x-1)x}; \tag{4.59}$$

$$Q_{\mathbf{p}}^2 = \frac{3}{2}\beta p_0 Q \; y(1-y). \tag{4.60}$$

In this case, if $Q = 0$ and $\beta \to \infty$, we will obtain the result for the non-thermal pure system. Now, let's consider $\varDelta m_{(3)}^2(\beta, q, \mu)|_{n,r\neq 0}$, which is given by

$$\begin{aligned}
\varDelta m_{(3)}^2(\beta, q, \mu)|_{n,r\neq 0} =& \frac{\lambda_R^2(\mu^2)^{4-d}}{32(4\pi)^d}\left(\frac{1}{\beta^2}\right)^{d-1}\int_0^1 \mathrm{d}x\mathrm{d}y \frac{((1-x)x)^{\frac{d-3}{2}}}{y^{\frac{d-1}{2}}}\int_0^\infty \mathrm{d}z\; z^{1-d} \\
&\times \exp\left[-\frac{\beta^2}{4\pi}\left(m_{eff}^2+\mathbf{p}_{eff}^2\right)z\right] \\
&\times \sum_{n,r\neq 0}\exp\left[-\frac{\pi}{z}\left(n^2+r^2\frac{x(x(y-1)+1)}{y}-2nrx\right)\right] \\
&\times \exp\left[-\beta p_0\left[i\left(rx(1-y)+ny\right)+\frac{3}{2}Q\; zy(1-y)\right]\right] \\
&\times \exp\left[i\pi Q\left(n(1-3y)+r(1+3x(y-1))\right)\right] \\
&\times \exp\left[\frac{\pi}{4}Q^2\left(\frac{x^2\left[-9y^2+10y-1\right]+x\left[9y^2-10y+1\right]+y}{(x-1)x}\right)z\right].
\end{aligned} \tag{4.61}$$

As we can see, the expression above is quite complicated to read. Now, we can perform some rearrangements to simplify it, and we obtain

$$\begin{aligned}
\varDelta m_{(3)}^2(\beta, q, \mu)|_{n,r\neq 0} =& \frac{\lambda_R^2(\mu^2)^{4-d}}{32(4\pi)^d}\left(\frac{1}{\beta^2}\right)^{d-1}\int_0^1 \mathrm{d}x\mathrm{d}y \frac{((1-x)x)^{\frac{d-3}{2}}}{y^{\frac{d-1}{2}}}\int_0^\infty \mathrm{d}z\; z^{1-d} \\
&\times \exp\left[-\frac{\beta^2}{4\pi}\left(m_{eff}^2+\mathbf{p}_{eff}^2\right)z\right]\sum_{n,r\neq 0}\exp\left[-\frac{\pi}{z}\left(n-\frac{i}{2}Q(1-3y)z\right)^2\right] \\
&\times \exp\left[-\frac{\pi}{z}C\left(r-\frac{i}{2}Q\;\frac{(1+3x(y-1))}{C}z\right)^2\right] \\
&\times \exp\left[-\beta p_0\left(i\left(rx(1-y)+ny\right)+\frac{3}{2}Q\; zy(1-y)\right)-\frac{\pi}{z}nrx\right] \\
&\times \exp\left[\frac{\pi}{4}Q^2\left(\frac{y}{(x-1)x}+4y-\frac{(1+3x(y-1))^2}{C}\right)z\right]
\end{aligned} \tag{4.62}$$

with

$$C = \frac{x(x(y-1)+1)}{y} \tag{4.63}$$

We can continue to rearrange (4.62) to obtain a form similar to (4.58). By doing this, we can achieve the following form

$$\begin{aligned}\Delta m^2_{(3)}(\beta,q,\mu)|_{n,r\neq 0} =&\frac{\lambda_R^2(\mu^2)^{4-d}}{32(4\pi)^d}\left(\frac{1}{\beta^2}\right)^{d-1}\int_0^1 \mathrm{d}x\mathrm{d}y\frac{((1-x)x)^{\frac{d-3}{2}}}{y^{\frac{d-1}{2}}}\int_0^\infty \mathrm{d}z\ z^{1-d}\\ &\times\exp\left[-\left(\frac{\beta^2}{4\pi}m^2_{eff}+Q_M^2\right)z\right]\\ &\times\exp\left[-\left(\frac{\beta^2}{4\pi}\mathbf{p}^2_{eff}+Q_{\mathbf{p}}^2\right)z\right]\\ &\times\sum_{n,r\neq 0}\exp\left[-\frac{\pi}{z}\left(n-Q_n z\right)^2\right]\\ &\times\exp\left[-\frac{\pi}{z}C\left(r-Q_r z\right)^2\right]\\ &\times\exp\left[-\beta p_0\left(i\left(rx(1-y)+ny\right)-\frac{\pi}{z}nrx\right)\right],\end{aligned}\tag{4.64}$$

where

$$Q_M^2=\frac{\pi}{4}Q^2\left(\frac{y}{(x-1)x}+4y-\frac{(1+3x(y-1))^2}{C}\right);\tag{4.65}$$

$$Q_n=\frac{i}{2}Q(1-3y);\tag{4.66}$$

$$Q_r=\frac{i}{2}Q\ \frac{(1+3x(y-1))}{C}.\tag{4.67}$$

As the only other possible divergence can occur with $n\neq 0$, $r=0$ or $n=0$, $r\neq 0$, we can examine the $r=0$ case. This implies that our mass correction term will be of the following form

$$\begin{aligned}\Delta m^2_{(3)}(\beta,q,\mu)|_{n\neq 0,r=0} =&\frac{\lambda_R^2(\mu^2)^{4-d}}{32(4\pi)^d}\left(\frac{1}{\beta^2}\right)^{d-1}\int_0^1 \mathrm{d}x\mathrm{d}y\frac{((1-x)x)^{\frac{d-3}{2}}}{y^{\frac{d-1}{2}}}\int_0^\infty \mathrm{d}z\ z^{1-d}\\ &\times\exp\left[-\left(\frac{\beta^2}{4\pi}m^2_{eff}+Q_M^2|_{r=0}\right)z\right]\\ &\times\exp\left[-\left(\frac{\beta^2}{4\pi}\mathbf{p}^2_{eff}+Q_{\mathbf{p}}^2\right)z\right]\\ &\times\sum_{n\neq 0}\exp\left[-\frac{\pi}{z}\left(n-Q_n z\right)^2-i\beta p_0 ny\right],\end{aligned}\tag{4.68}$$

where

$$Q_M^2|_{r=0}=\frac{\pi}{4}Q^2\left(\frac{y}{(x-1)x}+4y\right).\tag{4.69}$$

As we can see, if $Q=0$, we re-obtain the thermal case for the pure system, as presented in sec. 2.6. This expression is difficult to analyze, as all terms are mixed due to the nature of the sunset diagram. We will revisit this discussion in the next chapter.

# Chapter 5

# Conclusion

The study of classical and quantum fields in the presence of randomness has been a topic of research in the literature for decades. In this work, we focused on understanding the effects of disorder in a system at the broken symmetry phase and at low temperature. We started by investigating the effects of thermal fluctuations on the renormalized squared mass using the one-loop approximation, building upon recent work by Heymans [38]. Subsequently, we extended this study to the two-loop approximation.

Initially, we examined the effects of thermal fluctuations on the pure system and applied the low-temperature approach. Our results, obtained using analytic regularization, were consistent with the existing literature [37]. Building on these results, we then proceeded to derive the effects of disorder on the system. Given our focus on systems at the broken symmetry phase and low temperature, it was natural to consider disordered systems. We introduced the distributional zeta-function, which accounts for the effects of randomness in the action functional and leads to a non-local contribution associated with each momenta of the partition function.

The implications of disorder were particularly evident in the renormalized squared mass. Building on our results for the one-loop diagram, we extended our analysis to the two-loop diagram. We confirmed that the contributions from the double tadpole and double scoop diagrams, which are trivial cases, yielded the expected results. These contributions were straightforward to evaluate as they could be expressed in terms of the tadpole diagram, corresponding to the one-loop case. However, the evaluation of the non-trivial two-loop diagram proved to be more challenging. The interdependence of the third momentum and frequency with the internal and external momenta made the evaluation complex. The approach used in this study led to a complicated expression for this contribution, and it may be worthwhile to explore alternative methods to simplify the evaluation process.

In conclusion, this study sheds light on the effects of disorder in systems at the broken symmetry phase and low temperature. The renormalized squared mass serves as a key observable to understand these effects. While the evaluation of the two-loop diagram proved challenging, the results obtained for the trivial diagrams were in line with expectations. Further investigations and alternative approaches may provide insights into the evaluation of the non-trivial two-loop diagram and contribute to a more comprehensive understanding of the effects of disorder in these systems.

# Bibliography


[1] K. Binder and A. P. Young, Reviews of Modern physics **58**, 801 (1986).

[2] M. Mézard, G. Parisi, and M. A. Virasoro, *Spin glass theory and beyond: An Introduction to the Replica Method and Its Applications*, vol. 9 (World Scientific Publishing Company, 1987).

[3] C. De Dominicis and I. Giardina, *Random fields and spin glasses: a field theory approach* (Cambridge University Press, 2006).

[4] M. Mezard and A. Montanari, *Information, physics, and computation* (Oxford University Press, 2009).

[5] P. M. Ossi, *Disordered Materials: An Introduction* (Springer-Verlag, 2006).

[6] J. M. Ziman, *Models of disorder: the theoretical physics of homogeneously disordered systems* (Cambridge university press, 1979).

[7] S.-K. Ma, *Modern theory of critical phenomena* (Cambridge University Press, 1976).

[8] V. Dotsenko, *Introduction to the replica theory of disordered statistical systems* (Cambridge University Press, 2001).

[9] R. Brout, Physical Review **115**, 824 (1959).

[10] S. F. Edwards and P. W. Anderson, Journal of Physics F: Metal Physics **5**, 965 (1975).

[11] M. Mézard, G. Parisi, and M. Virasoro, Europhysics Letters **1**, 77 (1986).

[12] C. De Dominicis, Physical Review B **18**, 4913 (1978).

[13] B. Svaiter and N. Svaiter, International Journal of Modern Physics A **31**, 1650144 (2016).

[14] W. H. Zurek, U. Dorner, and P. Zoller, Physical review letters **95**, 105701 (2005).

[15] A. Zvyagin, Low Temperature Physics **42**, 971 (2016).

[16] M. Heyl, Reports on Progress in Physics **81**, 054001 (2018).

[17] M. Vojta, Reports on Progress in Physics **66**, 2069 (2003).

[18] G. O. Heymans and M. B. Pinto, Journal of High Energy Physics **2021**, 1 (2021).

[19] T. Vojta, Journal of Physics A: Mathematical and General **39**, R143 (2006).

[20] D. Belitz, T. Kirkpatrick, and T. Vojta, Reviews of modern physics **77**, 579 (2005).

[21] J. A. Hoyos and T. Vojta, Physical review letters **100**, 240601 (2008).

[22] T. Vojta, in *AIP Conference Proceedings* (American Institute of Physics, 2013), vol. 1550, pp. 188–247.

[23] T. Vojta, Annual Review of Condensed Matter Physics **10**, 233 (2019).

[24] T. Vojta, Physical review letters **90**, 107202 (2003).

[25] J. A. Hertz, in *Basic Notions of Condensed Matter Physics* (CRC Press, 2018), pp. 525–544.

[26] S. L. Sondhi, S. Girvin, J. Carini, and D. Shahar, Reviews of modern physics **69**, 315 (1997).

[27] S. Sachdev, *Quantum Phase Transitions* (Cambridge University Press, 2011).

[28] C. W. Bernard, Physical Review D **9**, 3312 (1974).

[29] L. Dolan and R. Jackiw, Physical Review D **9**, 3320 (1974).

[30] N. P. Landsman and C. G. Van Weert, Physics Reports **145**, 141 (1987).

[31] B. S. Kay, Physical Review D **20**, 3052 (1979).

[32] L. Ford and T. Yoshimura, Physics Letters A **70**, 89 (1979).

[33] D. J. Toms, Physical Review D **21**, 928 (1980).

[34] D. J. Toms, Physical Review D **21**, 2805 (1980).

[35] L. Ford and N. Svaiter, Physical Review D **51**, 6981 (1995).

[36] A. Malbouisson, J. Malbouisson, and A. E. d. Santana, Nuclear Physics B **631**, 83 (2002).

[37] H. Braden, Physical Review D **25**, 1028 (1982).

[38] G. Heymans, N. Svaiter, and G. Krein, Physical Review D **106**, 125004 (2022).

[39] M. Le Bellac, *Thermal field theory* (Cambridge university press, 2000).

[40] J. Drouffe and C. Itzykson, *Quantum field theory and statistical mechanics*, vol. 1 (Cambridge University Press, 1990).

[41] P. Ramond, *Field theory: a modern primer* (Addison Wesley, 1990).

[42] M. S. Swanson, *Path integrals and quantum processes* (Academic Press, 1992).

[43] M. Brown and M. Duff, Physical Review D **11**, 2124 (1975).

[44] G. Macfarlane, The London, Edinburgh, and Dublin Philosophical Magazine and Journal of Science **40**, 188 (1949).

[45] G. t Hooft, Nucl. Phys. B **61**, 455 (1973).

[46] J. C. Collins, Physical Review D **10**, 1213 (1974).

[47] T. Kaneyoshi, *Introduction to amorphous magnets* (World Scientific Publishing Company, 1992).

[48] B. D. Cullity and C. D. Graham, *Introduction to magnetic materials* (John Wiley & Sons, 2011).

[49] A. Bera, D. Rakshit, A. Sen, U. Sen, et al., Physical Review B **95**, 224441 (2017).

[50] A. N. Malmi-Kakkada, O. T. Valls, and C. Dasgupta, Physical Review B **90**, 024202 (2014).

[51] D. Belitz, T. R. Kirkpatrick, and T. Vojta, Physical Review Letters **84**, 5176 (2000).

[52] A. Lipowski, K. Gontarek, and D. Lipowska, Physical Review E **91**, 062801 (2015).

[53] M. E. Fisher, Physical Review **176**, 257 (1968).

[54] J. L. van Hemmen, Journal of Physics A: Mathematical and General **15**, 3891 (1982).

[55] A. C. van Enter and J. L. van Hemmen, Journal of statistical physics **32**, 141 (1983).

[56] J. L. van Hemmen and R. Palmer, Journal of Physics A: Mathematical and General **15**, 3881 (1982).

[57] E. Orlandini, M. Tesi, and S. G. Whittington, Journal of Physics A: Mathematical and General **32**, 469 (1999).

[58] E. Orlandini, M. Tesi, and S. Whittington, Journal of Physics A: Mathematical and General **33**, 259 (2000).

[59] E. Orlandini, M. Tesi, and S. Whittington, Journal of Physics A: Mathematical and General **35**, 4219 (2002).

[60] R. Martin, M. S. Causo, and S. G. Whittington, Journal of Physics A: Mathematical and General **33**, 7903 (2000).

[61] D. L. Stein and C. M. Newman, *Spin glasses and complexity*, vol. 4 (Princeton University Press, 2013).

[62] V. S. Dotsenko, M. Feigel'man, and L. Ioffe, *Spin glasses and related problems*, vol. 1 (CRC Press, 1991).

[63] L. F. Cugliandolo, arXiv preprint cond-mat/0210312 (2002).

[64] E. Ising, Ph.D. thesis, Grefe & Tiedemann Hamburg (1924).

[65] S. Kirkpatrick and D. Sherrington, Physical Review B **17**, 4384 (1978).

[66] A. Larkin, Sov. Phys. JETP **31** (1970).

[67] Y. Imry and S.-k. Ma, Physical Review Letters **35**, 1399 (1975).

[68] A. Young, Journal of Physics C: Solid State Physics **9**, 2103 (1976).

[69] G. Parisi and R. Shankar, *Statistical field theory* (Addison-Wesley, 1988).

[70] K. Binder, Zeitschrift für Physik B Condensed Matter **50**, 343 (1983).

[71] M. Aizenman and J. Wehr, Physical review letters **62**, 2503 (1989).

[72] J. Bricmont and A. Kupiainen, Communications in mathematical physics **116**, 539 (1988).

[73] J. Bricmont and A. Kupiainen, Physical review letters **59**, 1829 (1987).

[74] J. Verbaarschot and M. Zirnbauer, Journal of Physics A: Mathematical and General **18**, 1093 (1985).

[75] M. R. Zirnbauer, arXiv preprint cond-mat/9903338 (1999).

[76] V. Dotsenko, Philosophical Magazine **92**, 16 (2012).

[77] T. Tanaka, Interdisciplinary information sciences **13**, 17 (2007).

[78] J. L. van Hemmen and R. G. Palmer, Journal of Physics A: Mathematical and General **12**, 563 (1979).

[79] P. Charbonneau, arXiv preprint arXiv:2211.01802 (2022).

[80] G. Parisi and V. Dotsenko, Journal of Physics A: Mathematical and General **25**, 3143 (1992).

[81] R. J. A. Diaz, Ph.D. thesis, Centro Brasileiro de Pesquisas Físicas (2018).

[82] M. Abramowitz and I. A. Stegun, *Handbook of Mathematical Functions* (Dover Publications, 1972).

[83] I. Gel'fand and G. Shilov, *Generalized Functions: Properties and Operations, Volume 1* (ACADEMIC PRESS, 1964).